의학박사 학위논문

Thermo- and chemosensory cation channel TRPV1: a novel target for skin anti-aging

열 및 화학 자극으로 활성화되는 양이온통로인 TRPV1 을 표적으로 하는 피부항노화 연구

2013 년 12 월

서울대학교 대학원

의과학과 의과학전공

강 소 민

A thesis of the Degree of Doctor of Philosophy

열 및 화학 자극으로 활성화되는 양이온통로인 TRPV1 을 표적으로 하는 피부항노화 연구

Thermo- and chemosensory cation channel TRPV1: a novel target for skin anti-aging

December 2013

Department of Biomedical Sciences,

Seoul National University College of Medicine

So Min Kang

열 및 화학 자극으로 활성화되는 양이온통로인 TRPV1을 표적으로 하는 피부항노화 연구

지도교수 정 진 호

이 논문을 의학 박사 학위논문으로 제출함

2013년 12월

서울대학교 대학원
의과학과 의과학전공
강 소 민

강소민의 의학박사 학위논문을 인준함

2013년 12월

위 원 장 김 규 한 (인)

부위원장 정 진 호 (인)

위 원 박 동 은 (인)

위 원 김 성 준 (인)

위 원 오 상 호 (인)

Thermo- and chemosensory cation channel TRPV1: a novel target for skin anti-aging

by

So Min Kang

(Directed by Jin Ho Chung MD, PhD)

A thesis submitted to the Department of Biomedical Sciences in partial fulfillment of the requirements for the Degree of Doctor of Philosophy in Medical Sciences at Seoul National University College of Medicine

December 2013

Approved by Thesis Committee:

Professor Kyu Han Kim Chairman

Professor Jin Ho Chung Vice chairman

Professor Dongeun Park

Professor Sung Joon Kim

Professor Sang Ho Oh

ABSTRACT

Transient receptor potential vanilloid 1 (TRPV1) is a member of the non-selective cationic channel family. TRPV1 is activated by capsaicin, heat, ultraviolet (UV), and acid, and its activation results in an influx of divalent and monovalent cations such as Ca^{2+}, Na^{+}, and Mg^{2+} ions.

TRPV1 channel is expressed not only in neuronal cells in the brain, but also in keratinocytes in the epidermis. Recent studies suggested that TRPV1 regulates the heat- and UV-induced matrix metalloproteinases-1 (MMP-1) expression in human keratinocytes *in vitro*. In addition, the expression level of TRPV1 proteins was increased by heat and UV stimulus in human skin *in vivo*. However, little is known about the initial mechanism of UV-induced TRPV1 activation. It is important to study the initial activation mechanism of TRPV1 by UV irradiation in order to identify the precise role of TRPV1 in UV-induced responses. In the present study, I investigated how UV can activate TRPV1 through the non-receptor protein tyrosine kinase Src in HaCaT keratinocytes. UV-irradiation induced TRPV1 and Src trafficking into cell surface membrane in HaCaT cells. This UV-induced trafficking of TRPV1 was also blocked by Src inhibition. These results suggest that UV induces TRPV1 trafficking into cell membrane through Src kinase activation, and this initial process leads to the subsequent reactions including UV-

induced MMP-1 and pro-inflammatory cytokine expressions.

Based on these functional role and basal mechanism of TRPV1 following photo-stimulus, TRPV1 can be a novel target for anti-skin aging. In this study, I investigated the activity of the TRPV1 inhibitory peptide (TIP) as a novel blocker for anti-skin aging, and observed the beneficial effect of TIP in UV-induced responses both *in vitro* and *in vivo* system.

According to recent studies, TRPV1 may be related to intrinsic skin aging. TRPV1 protein was expressed more in the sun-protected (upper-inner arm) skin of the elderly than in that of the young. The increased TRPV1 expression in the aged skin implies that TRPV1 may be related to well-known skin conditions of the elderly, such as senile pruritus or neurogenic inflammation, as well as to the change of neuronal outgrowth by aging. In this study, it was observed that the expression patterns of several neuronal outgrowth factors including TRPV1 are changed by aging using microarray analysis from the young and aged skin.

In conclusion, Src-mediated activation of epidermis-expressed TRPV1 may have a critical role in heat or UV-induced responses, and increased expression of TRPV1 and neuronal outgrowth factors in aged skin may be related to senile skin symptoms. Therefore, TIP may act as a novel anti-skin aging molecule.

Keywords: TRPV1, Intrinsic aging, neuronal outgrowth factors, UV-

induced responses, TRPV1 inhibitory peptide (TIP), Src tyrosine kinase

Student number: 2010-30603

CONTENTS

LIST OF TABLES

LIST OF FIGURES

INTRODUCTION

Life expectancy is the best interest of human history, and it has been increased geometrically worldwide in recent years. Subsequently, researches on skin aging have been continuously and markedly increased.

Skin Aging

Skin aging is a continuous process that results in several morphological and functional changes in the skin. The changes of epidermis involve thinning of stratum spinosum and flattening of the junction between epidermis and dermis. Dermal changes involve degradation of collagen and elastic fibers which are essential for stability and tensile strength [1].

Skin aging involves two processes, intrinsic aging and photoaging [1-3]. Intrinsic aging is caused by slow, irreversible tissue degeneration and represented by smooth, pale, and finely wrinkled skin [3-5], while photoaging is mainly caused by the ultraviolet (UV) exposure and characterized by coarsely wrinkled skin, with dyspigmentation and telangiectasia [2, 5-11]. Intrinsically aged skin and photoaged skin have distinct features morphologically and histologically. Nevertheless, many observations and studies have shown that both aging processes involve

very similar biochemical, biological, and molecular mechanisms [3, 5, 9] In both chronologically aged and photoaged skin, activator protein-1 (AP-1) is elevated and the activity and expression of matrix metalloproteinases (MMP) are increased, followed by more degradation of collagen as compared to young skin [9-12]. In addition, synthesis of types I and III procollagen is decreased in chronologically aged and photoaged skin [13-15]. By the increase of collagen degradation and decrease of new collagen synthesis, an overall collagen levels in the dermis are reduced. It seems that photoaging exhibits exacerbated and amplified changes associated with chronologic skin aging [16-18].

Photoaging

Solar UV-irradiation damages human skin and causes premature skin aging (photoaging) characterized by thickening, rough texture, coarse wrinkles, and mottled pigmentation [4, 5]. Photoaging induced by UV-irradiation is progressed primarily by disorganization of collagen fibrils [11] comprising most of skin connective tissues and accumulation of abnormal, amorphous, elastin-containing materials [2, 19]. As collagen fibers and elastin fibers are responsible for the strength and elasticity of skin [19], their disarrangement by photoaging causes skin to appear aged [6].

MMPs

Collagen degradation is partly related to the presence of MMPs, which are secreted by epidermal keratinocytes and dermal fibroblasts. MMPs, a family of structurally related matrix-degrading enzymes, play important roles in various destructive processes, including inflammation [20], tumor invasion [21], and skin aging [14, 22]. It has been reported that increased expression of some MMPs is responsible for the enhanced destruction of dermal collagen during intrinsic skin aging and UV-induced photoaging [11]. MMPs are expressed at low levels in unstimulated cells, but some are induced by various extracellular stimuli, including growth factors, cytokines, tumor promoters, and ultraviolet and infrared radiation [20, 21]. Although the signaling mechanism remains unclear, UV radiation somehow triggers DNA binding of AP-1, which induces MMPs, such as collagenase (MMP-1), stromelysin (MMP-3), gelatinase (MMP-9), and metalloelastase (MMP-12) [22]. Once collagen is cleaved by MMP-1, it is further degraded by MMP-2 and MMP-9, which are also induced by exposure to UV light [23]. Rodents lack the MMP-1 gene, instead, it is functionally replaced by MMP-13 in these animals [24].

TRPV1

Transient receptor potential vanilloid 1 (TRPV1) is a member of a non-selective cationic channel family; activation of TRPV1 induces an influx of divalent cations (i.e., Ca^{2+} and Mg^{2+}). TRPV1 is inhibited by a specific antagonist such as capsazepine and 5'-iodoresiniferatoxin (5'-I-RTX) [23-26]. TRPV1 can be directly activated by vanilloids, exposure to UV, heat or protons (reduced pH), and conditions that occur during tissue injury [27], thus implicating the channel as a primary cellular sensor to thermal or chemical stimulation. The presence of TRPV1 has recently been reported in various tissues, such as brain [28, 29], kidney [29], bronchial epithelial cells [30], and even in keratinocytes in the epidermis [31].

TRPV1 and photoaging

Recently, it was suggested that TRPV1 regulates heat shock-induced MMP-1 expression in human epidermal keratinocytes [32, 33]. Heat shock induced the expression of MMP-1 mRNA and protein in HaCaT cells and normal human epidermal keratinocytes (NHEK) [34]. Treatment with TRPV1 inhibitors or knockdown of TRPV1 decreased heat shock-induced MMP-1 expression in HaCaT cells [35]. It was also reported that heat shock induced calcium influx through TRPV1 plays a

significant role in the heat shock-induced MMP-1 expression in HaCaT cells, and which is mediated by activated TRPV1 through the calcium dependent protein kinase C-alpha (PKC-α) signaling pathway in human keratinocytes [35, 36]. It is also found that acute heat shock induced TRPV1 expression in human skin [35].

Our previous study suggests that calcium influx through TRPV1 is critical for UV-induced MMP-1 expression in immortalized human epidermal keratinocytes, HaCaT cells, and a calcium-dependent PKC is involved in the signaling cascade [37]. UV-irradiation induced calcium influx and increased membrane current, which is inhibited by treatment with TRPV1 inhibitors (capsazepine and ruthenium red). These TRPV1 inhibitors prevented UV-induced MMP-1 expression in HaCaT cells. Both UV-induced increases in $[Ca^{2+}]_i$ and MMP-1 were suppressed by a calcium-dependent PKC inhibitor. These studies support that epidermal TRPV1 seems to function as a sensor for noxious stimulus such as UV or heat. In this respect, TRPV1 may be a target for preventing skin photoaging most commonly caused by repeated UV light exposure [37].

TRPV1 and intrinsic skin aging

Skin aging is a complicated process resulted from the passage of time. A recent study describes that the expression level of TRPV1 is increased in

the aged human skin *in vivo*. Both protein and mRNA of TRPV1 were expressed at higher levels in sun-protected skin of the elderly than in that of the young [38, 39]. These results suggest that TRPV1 seems to be related to the development of intrinsic aging of human skin.

According to David A. Greenberg, TRPV1 is related to adult neurogenesis [40]. Cannabinoid receptor (CBR) is well known as a regulating factor for adult neurogenesis [40]. Cannabinoid receptor 1 (CB1R) knock-out mice have been well studied in an adult neurogenesis model. Neurogenesis is defective in mice lacking CB1R, suggesting that endogenous signaling through CB1R induces basal levels of neurogenesis *in vivo* [41-43]. The group of David A. Greenberg provided that both CB1R and TRPV1 regulate adult neurogenesis *in vivo*, as measured by the increased incorporation of bromodeoxyuridine (5-bromo-2'-deoxyuridine, BrdU) into cells that are located in neuroproliferative zones of the brain and that express neuronal lineage marker proteins [40]. Based on these results that both CB1R and TRPV1 cooperatively regulate adult neurogenesis, I hypothesized that increased expression level of TRPV1 in epidermal skin is thought to be related to adult neurogenesis. Therefore I investigated the expression level of CBRs including CB1R and CB2R in the aged human skin compared to the young skin. Additionally, I also investigated the well-known neurogenetic factors including nerve growth factor (NGF) and brain-derived

neurotrophic factor (BDNF) [44-49]. Since the amount of neurofilaments is a significant indicator for neuronal outgrowth [50-52], I examined the neurofilament protein levels in both young and aged human skin by measuring 68 kDa neurofilament light chain (NF 68), 200 kDa neurofilament heavy chain (NF 200) [53, 54]as well as a well-known neurofilament marker, protein gene product 9.5 (PGP 9.5) [55-57].

Activation mechanism of TRPV1

TRPV1 protein has been identified to have many regions and amino acids related to specific functions including phosphorylation, capsaicin action, proton action, heat activation, multimerization, desensitization, and permeability [26, 58]. There are several molecules to phosphorylate TRPV1, such as protein kinase C (PKC), Ca^{2+}/calmodulin-dependent protein kinase (CaMKII), and proto-oncogene tyrosine kinase Src [59-63].

Phosphorylation of TRPV1 occurs downstream by activation of Gq-coupled receptors by several inflammatory factors including bradykinin, prostaglandins, ATP, trypsin or tryptase [64-72]. Phosphorylation of TRPV1 by PKC not only potentiates capsaicin- or proton-evoked responses, but also reduces the temperature threshold for TRPV1 activation. Then normal body temperature range, which do not evoke

pain in normal circumstances, is capable of activating TRPV1, which leads to the sensation of pain. Three target residues phosphorylated by PKC in TRPV1 include Ser residues (Ser 502 and Ser 800) and Thr residue (Thr 705) [61, 73, 74]. When these residues were replaced with Ala, the potentiation of TRPV1 activity induced by several stimuli such as capsaicin, proton, or heat was blocked [74].

Another molecule, CaMKII regulates TRPV1 activity upon phosphorylation of TRPV1 at Ser 502 and Thr 705 by regulating capsaicin binding [75]. It is well known that calcineurin, calcium-dependent serine-threonine phosphatase, inhibits the desensitization of TRPV1, which indicates that a phosphorylation/dephosphorylation process is important for TRPV1 activity [58, 74-76]. Moreover, recent findings suggest that TRPV1 plays an important role in the signaling pathway of UV-induced MMP-1 expression, and it seems to be mediated by calcium-dependent PKC and CaMKII in HaCaT cells [37].

A recent study demonstrates that Src kinase phosphorylates the Tyr residue (Tyr 200) of TRPV1, which play a significant role in the mechanism of TRPV1 trafficking. NGF induces rapid sensitization of TRPV1 by the phosphorylation Tyr 200 by Src [63].

The phosphorylation of TRPV1 by three different kinases seems to control TRPV1 activity through the dynamic balance between the phosphorylation and dephosphorylation.

Therefore blocking these functional residues, for example by synthesizing peptides mimicking these sites for competitive inhibition, could be a very useful strategy for the development of novel anti-skin aging or anti-nociceptive agents.

Trafficking of TRPV1 into cell membrane and Src kinase

Membrane current is enhanced through TRPV1 heat-gated ion channel by various pro-inflammatory factors such as bradykinin, ATP, and NGF, which called sensitization or hyperalgesia process, and then the sensitivity to noxious stimulus like heat is enhanced [77, 78]. Several mechanisms for the sensitization of TRPV1 have been suggested, and the trafficking of TRPV1 from cytosolic region to the surface membrane is one of them [79, 80]. Src tyrosine kinase phosphorylates a single tyrosine residue, Y200, on TRPV1 and mediates TRPV1 trafficking to the surface membrane [63].

Based on these results, I investigated that the sensitization of TRPV1 to the other noxious stimulus, UV-irradiation, is mediated by Src tyrosine

kinase. Besides, I examined whether the localization of TRPV1 was changed by UV-irradiation, from cytosolic region to surface membrane, and whether this process was mediated by Src tyrosine kinase.

Potential of TRPV1 blocker

As TRPV1 plays an important role in UV-induced skin photoaging process, it could be a significant target for prevention of skin photoaging. Although there are many inhibitors for TRPV1, they are too toxic to apply on the human skin. Therefore, it is necessary to develop a novel inhibitor blocking the activity of TRPV1 safely for anti-skin-photoaging. As a strategy for inhibition of TRPV1 activity, the single amino acid residue, Thr 705, was considered. Thr 705 residue on TRPV1 is phosphorylated by PKC and CaMKII, followed by conformational change and gate-open of TRPV1 channel. As a strategy to block this site, I synthesized a 9-sequence-peptide mimicking this region including Thr 705, 701-709 residues for a competitive inhibition (Fig. 1). Since a peptide agent is relatively simple, non-harmful, and non-toxic, and easy to produce, it has been widely employed in the cosmetic industry for anti-skin aging [81-83]. For instance, a fragment of pro-collagen I (KTTKS) is a well-known topical peptide, which increases dermal matrix production in fibroblasts. The permeability of peptide into the skin depends on the ionic nature of such materials, and it has to be tested both *in vitro* and *in vivo* studies [84-86].

I investigated whether this novel TRPV1 blocker, TRPV1 Inhibitory Peptide$^{701-709}$ (TIP) can inhibit UV-induced MMP-1 or pro-inflammatory cytokine expression and a calcium influx in HaCaT cells. Additionally, I investigated the effect of TIP in UV-induced responses including skin thickness, MMP-13 expression, and apoptosis using hairless mice.

TRPV1 and itch

Pruritus is an irritating sensation which provokes a desire to scratch. It is one of the most common symptoms in various skin and systemic diseases including contact dermatitis, atopic dermatitis, cholestasis, and chronic renal failure. Pruritus is also related to aging. So many elderly people frequently suffer from pruritus [87-91]. Nevertheless, any definite cause of senile pruritus is not sufficient and there is no effective therapy to treat this symptom.

The sensation is induced by several endogenous substances such as histamine, substance P (SP), vasoactive intestinal peptide and neurotensin [92-95]. For many years histamine has been well-known as a major itch-inducing factor. And the blockers inhibiting histamine receptors, has been used to treat pruritus [96-99]. However, it is suggested recently that SP is also a very potent pruritogenic endogenous neuropeptide and related to various pruritic diseases [95, 100]. Another

study demonstrated that treatment of SP to the skin induces scratching without histamine-afferent effects in mice, and suggested that SP-induced itch is histamine-independent mechanism [93].

It has been well described that TRPV1 ion channels expressed in keratinocytes are activated by the external stimulus including heat exposure, and from the keratinocytes expressing TRPV1, pro-inflammatory and pruritic mediators are released, followed by the paracrine signaling to adjacent afferents leading to neuronal activation [62, 67-69]. Sensitizing and activating mediators in the skin target receptors on primary afferent nerve fibers involved in itch and pain processing. TRPV1 activation affects the release of pruritogenic cytokine mediators from these non-neuronal cells [101-103]. Moreover, it has been found that SP is released from sensory nerves, followed by TRPV1 activation, leading to stimulation of neurokinin 1 receptors (NK1R) on epithelial cells, and reactive oxygen species (ROS) generation [104, 105]. Therefore, the result of increased TRPV1 expression in aged skin [38, 39] implies that TRPV1 may play an important role in the pathophysiology of the skin symptoms related to aging, such as pruritus occurring in elderly subjects [106-108]. In this study, I investigated whether pruritogenic factor, substance P, known as TRPV1 downstream signaling molecule, is also increased in intrinsically aged skin. Additionally, I investigated the expression level of the receptor of substance P, neurokinin 1 receptor

(NK1R), in young and aged human skin. I also investigated whether activation of TRPV1 induces NK1R expression in HaCaT cells.

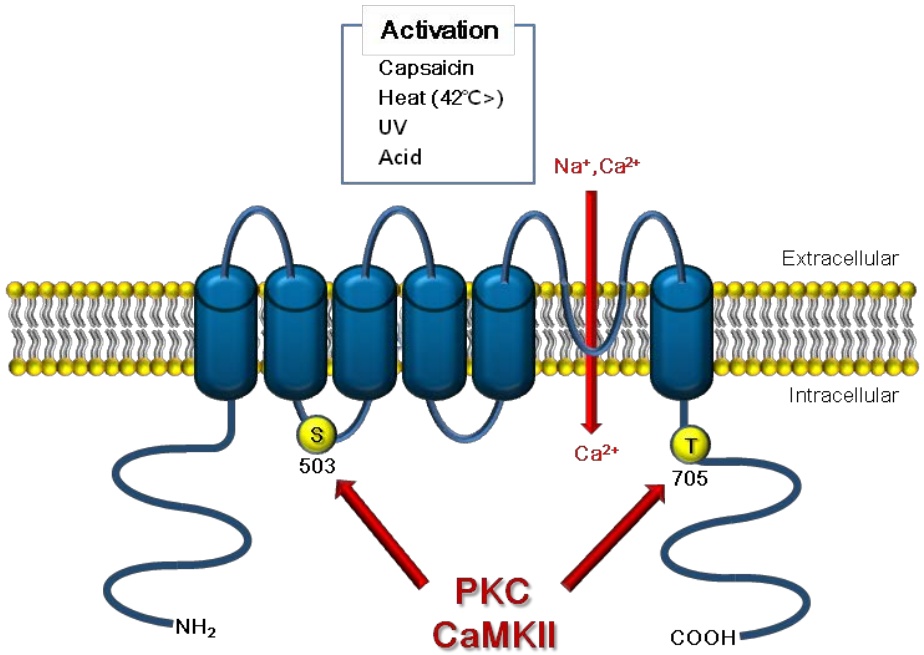

QRAITILDT

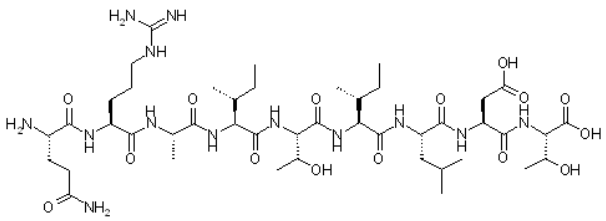

TRPV1 inhibitory peptide$^{701-709}$ (TIP) in both human and mouse

Figure 1. TRPV1 inhibitory peptide (amino acid sequence: 701-709) design

TRPV1 is phosphorylated by protein kinases such as protein kinase C (PKC) and Ca^{2+}/calmodulin-dependent protein kinase (CaMKII) which lead to its structural transformation and channel open. Based on this, a

novel peptide mimicking the C-terminal amino acid sequences of human TRPV1 (a.a 701-709: QRAIT<u></u>ILDT) was synthesized, the sequences of which are phosphorylated by both PKC and CaMKII. These sequences in human TRPV1 are identical with those in mouse TRPV1.

PURPOSES

The capsaicin-gated ion channel TRPV1 play a significant role in both photo- and intrinsic skin aging. Therefore, it is very worth that indentifying of the TRPV1 activation mechanism in UV-induced signaling and finding out a novel inhibitory substance targeting TRPV1 for skin anti-aging. Additionally, to study about the meaning of TRPV1 increase in intrinsic aging is also a valuable thing.

Chapter I. UV-induced TRPV1 trafficking into cell membrane is mediated by Src tyrosine kinase.

This chapter had two objectives : to investigate (1) whether TRPV1 is trafficked to cell surface membrane as an initial UV-induced responses; and (2) whether UV-induced TRPV1 trafficking is regulated by Src tyrosine kinase.

Chapter II. A synthetic peptide targeting TRPV1 inhibits UV-induced responses in HaCaT cells and in mouse skin.

Although there are several inhibitor of TRPV1, since they are too toxic to apply on human skin, it is necessary to develop a non-toxic novel blocker targeting TRPV1. This chapter had two objectives : to investigate (1) whether a novel blocker, TRPV1 inhibitory peptide (TIP) has an inhibitory effect on UV-induced MMP-1 or pro-inflammatory cytokines expression in HaCaT cells; and (2) whether TIP has also an inhibitory effect on UV-induced responses in mouse model.

Chapter III. Microarray analysis reveals the increased expression of nervous system-related genes in the aged human skin.

Finally, to study the meaning of TRPV1 increase in intrinsic skin aging, I investigated the expression level of several well-known neurite outgrowth factors related with TRPV1 and substance P, the itch related-downstream signaling molecule of TRPV1, in both young and aged human skin.

Chapter I.

UV-induced TRPV1 trafficking into cell membrane is mediated by Src tyrosine kinase.

ABSTRACT

Transient receptor potential vanilloid 1 (TRPV1) channel can be activated by vanilloids, exposure to ultraviolet (UV) light, heat, protons, and conditions that occur during tissue injury. In the present study, I investigated how UV could activate TRPV1 through the non-receptor protein tyrosine kinase Src in HaCaT keratinocytes. UV-induced expressions of MMP-1 and pro-inflammatory cytokines, including TNF-α, IL-6, and IL-8, were inhibited by pretreatment with a Src kinase inhibitor, PP2, in HaCaT cells, and this inhibition was partially recovered by treatment with a TRPV1 agonist, capsaicin. Confocal microscopy revealed that UV-irradiation induced TRPV1 and Src trafficking into cell membrane in HaCaT cells at 5 minutes, resulting in their co-localization. At 15 minutes, Src kinase moved back to cytoplasm, while TRPV1 was still remained in the cell membrane. This UV-induced trafficking of TRPV1 was also blocked by treatment with PP2. These results suggest that UV induces TRPV1 trafficking into cell membrane, which is involved in UV-induced expressions of MMP-1 and pro-inflammatory cytokines, and is mediated by Src kinase activity.

Keywords: TRPV1, UV-irradiation, Src tyrosine kinase, membrane trafficking

MATERIALS AND METHODS

Materials

PP2 (a selective inhibitor of Src-family tyrosine kinases, P0042), Capsaicin (TRPV1 agonist, M2028), and wheat germ agglutinin (WGA, membrane specific marker, FITC-conjugated, L4895) were purchased Sigma-Aldrich (St. Louis, MO). Anti-human MMP-1 antibody was acquired from Lab Frontier (Seoul, Korea). Goat polyclonal antibody against TRPV1 (sc-12498) and Goat polyclonal antibody against actin (sc-1616) were supplied by Santa Cruz Biotechnology (Santa Cruz, CA). Rabbit polyclonal antibody against Src tyrosine kinase (# 2108) and rabbit polyclonal antibody against phospho-Src (Tyr 416, # 2101) were purchased from Cell Signaling technology, Inc (Danvers, MA). Mounting solution with DAPI (VECTASHIELD Mounting Media for Fluorescence, H1200) was acquired from VECTOR Laboratories (Burlingame, CA). Donkey anti-goat IgG Alexa Fluor® 488 (A11055), donkey anti-goat IgG Alexa Fluor® 594 (A-11014), and goat anti-rabbit IgG Alexa Fluor® 594 (A-11012) were acquired from Life technologies (Rockville, MD). The cell culture media and antibiotics were purchased from Life Technologies (Rockville, MD). Fetal bovine serum (FBS) was obtained from Hyclone (Logan, UT).

Methods

1. Cell culture and treatments

The immortalized human keratinocytes cell line, HaCaT, was cultured in Dulbecco's modified Eagle's media (DMEM) supplemented with glutamine (2 mM), penicillin (400 U/ml), streptomycin (50 mg/ml), and 10% FBS at 37°C in a humidified atmosphere containing 5% CO_2. For treatment, the cells were cultured to 80% confluence and then maintained in culture media without FBS for 24 hours. The cells were washed with phosphate buffered saline (PBS) and irradiated with UV. After UV treatment, the culture medium was replaced with fresh medium without FBS, and the cells were further incubated for 48 hours in Western blot analysis and for 5 minutes or 15 minutes in immunofluorescence experiment. PP2 or capsaicin was added 30 minutes before UV treatment, and incubated for 48 hours after UV treatment.

2. UV-irradiation

In the Western blot and immunofluorescence experiments, the HaCaT cells were irradiated with a Philips TL 20W/12 RS fluorescent sun lamp with an emission spectrum ranging between 275 and 380 nm (peak, 310–315 nm) [27]. A Kodacel filter (TA401/407; Kodak) was used to block

UVC, which has wavelengths of <290 nm. The UV strength (irradiated with 75 mJ/ cm^2) was measured using a Waldmann UV meter (model 585100).

3. Western blot analysis

In order to determine the amounts of MMP-1 secreted into the culture media, equal aliquots of conditioned culture media from an equal number of cells were fractionated by 10% SDS–PAGE, transferred to a Hybond ECL membrane (Amersham Biosciences, Buckinghamshire, England), and analyzed by Western blotting with a rabbit monoclonal antibody against MMP-1 (Lab Frontier) by enhanced chemiluminescence (Amersham Biosciences). As controls, the levels of the corresponding β-actin were determined in the same cell lysates using the antibodies for β -actin (Santa Cruz Biotechnology, Santa Cruz, CA). The signal strengths were quantified using a densitometric program (TINA; Raytest Isotopenme b gerate, Straubenhardt, Germany).

4. Enzyme-linked immunosorbent assay (ELISA)

Protein levels of IL-6, IL-8, and TNF-α secreted into culture media from HaCaT cells were measured by ELISA or human Fuorokine Multi

Analyte Profiling (MAP) bead-based assays, according to the manufacture's protocol (R&D systems, MN, USA) using Versamax ELISA reader (Molecular Devices, CA, USA) or Bioplex200 (Bio-rad) system, respecively.

5. Immunofluorescence

For immunofluorescence staining, the HaCaT cells were seeded in 4-well chamber slides (Falcon, BD Biosciences, Bedford, MA) with 1.5 x 10^4 cells per well and incubated for 24 hours. FITC-conjugated WGA was treated for 30 minutes. Cells were fixed in 4% paraformaldehyde in phosphate-buffered saline (PBS) for 30 minutes. Fixed cells were blocked with blocking solution (10% goat serum, 0.5% gelatin and 0.1% Triton X-100 in PBS) for 30 minutes and then incubated with primary antibodies such as goat polyclonal antibody against TRPV1 or rabbit polyclonal antibody against Src tyrosine kinase diluted with blocking solution for overnight. The primary antibody treated cells were washed 3 times with PBS and incubated with fluorescein-conjugated secondary antibodies (Alexa Fluor®) diluted in blocking solution for 1 hour. Subsequently, the coverslips were mounted onto slides after the treatment of mounting solution with DAPI. Cells were observed under the fluorescence

microscope (Carl Zeiss, Jena, Germany). Specimens were visualized with 405, 488, 545 nm lasers

RESULTS

UV-induced MMP-1 and pro-inflammatory cytokines expressions are regulated by Src tyrosine kinase in HaCaT cells.

To investigate whether Src tyrosine kinase regulates UV responses, the expression level of UV-induced MMP-1 and pro-inflammatory cytokines were measured in the presence or absence of Src inhibitor (Fig. 2). HaCaT cells were exposed to UV (at 75 mJ/cm^2), and the level of secreted MMP-1 was measured in culture media at 48 hours after UV-irradiation. UV-irradiation increased the level of MMP-1 protein expression, and pretreatment of HaCaT cells with Src kinase inhibitor, PP2, decreased the UV-induced MMP-1 expression compared with the UV-irradiated group (Fig. 2A). And I measured the protein level of pro-inflammatory cytokines with ELISA, and the protein level of IL-6, IL-8, and TNF-α were increased by UV-irradiation compared to the control group (1121.3±112.5%, 613.4±94.2%, 352.1±72.3% of the control group, respectively; The data shown are representative of three independent experiments, Fig. 2B, 2C, 2D). Pretreatment of PP2 decreased the UV-induced IL-6 expression in a dose-dependent manner (compared to the UV-irradiated group (757.7±101.2%, 672.5±135.4%, 548.2±136.2% of the

control group by 2.5, 5, and 10 μM, respectively; The data shown are representative of three independent experiments, Fig. 2B). Pretreatment of PP2 decreased the UV-induced IL-8 expression in a dose-dependent manner (compared to the UV-irradiated group (443.0±75.8%, 263.8±52.7%, 170.4±31.2% of the control group by 2.5, 5, and 10 μM, respectively; The data shown are representative of three independent experiments, Fig. 2C). Besides, the UV-induced TNF-α expression was decreased by PP2 pretreatment in a dose-dependent manner (compared to the UV-irradiated group (305.9±12.5%, 280.7±73.2%, 203.4±35.4% of the control group by 2.5, 5, and 10 μM, respectively; The data shown are representative of three independent experiments, Fig. 2D).

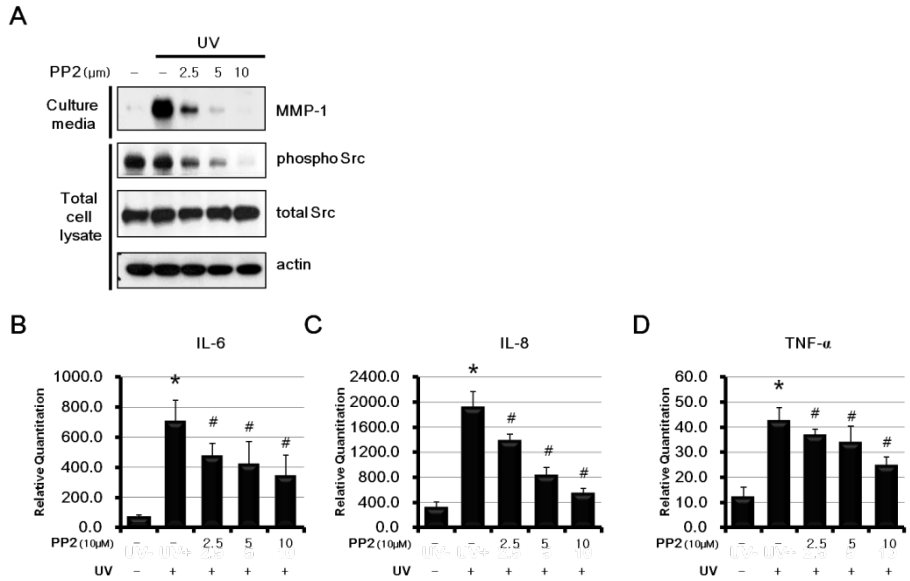

Figure 2. Src regulates UV-induced MMP-1 and pro-inflammatory cytokine expression.

HaCaT cells were cultured in 60 mm dish. Culture media was changed with serum-free media and incubated for 24 hours. After pretreatment with the specific Src inhibitor, PP2, for 30 minutes, the cultured HaCaT cells were irradiated with UV (75 mJ/cm^2). Fresh media containing PP2 was added, and the cells were further incubated for 48 hours. The amounts of MMP-1 released into the culture media and phospho-Src, and total-Src protein from total cell lysates were determined by Western blotting (Fig. 2A). The protein levels of IL-6, IL-8, and TNF-α were analyzed by ELISA (Fig. 2B, 2C, 2D). Results are expressed as mean

values ± standard error (SE). *P < 0.05 versus UV-untreated control group. $^{\#}$P < 0.05 versus UV-treated group.

Inhibitory effect by PP2 in UV-induced responses is partially recovered by TRPV1 agonist.

To investigate whether TRPV1 is related to these UV responses mediated by Src tyrosine kinase, the expression level of UV-induced MMP-1 and pro-inflammatory cytokines were measured after treatment with TRPV1 agonist, capsaicin (Fig. 3). HaCaT cells were exposed to UV (at 75 mJ/cm^2), and the level of secreted MMP-1 was measured in culture media at 48 hours after UV-irradiation. UV-irradiation increased the level of MMP-1 protein expression, and pretreatment of HaCaT cells with Src kinase inhibitor, PP2, decreased the UV-induced MMP-1 expression compared with the UV-irradiated group (Fig. 3A).

And I measured the protein level of pro-inflammatory cytokines with ELISA analysis, and the protein level of IL-6, IL-8, and TNF-α were increased by UV-irradiation compared to the control group (392.8±35.2%, 365.6±80.2%, 1783.0±300.2% of the control group, respectively; The data shown are representative of three independent experiments, Fig. 3B, 3C, 3D). Pretreatment of 5 μM of PP2 decreased the UV-induced IL-6, IL-8, and TNF-α expression levels compared to the UV-irradiated group (152.0±39.4%, 45.85±69.5%, 577.8±299.4% of the control group, respectively; The data shown are representative of three independent experiments, Fig. 3B, 3C, 3D). These decreases by treatment with PP2

were recovered by pretreatment of capsaicin at 5 μM of concentration compared to the UV-irradiated and PP2-treated control group (233.3±41.5%, 112.4±72.4%, 1567.4±289.7% of the control group, respectively; The data shown are representative of three independent experiments, Fig. 3B, 3C, 3D).

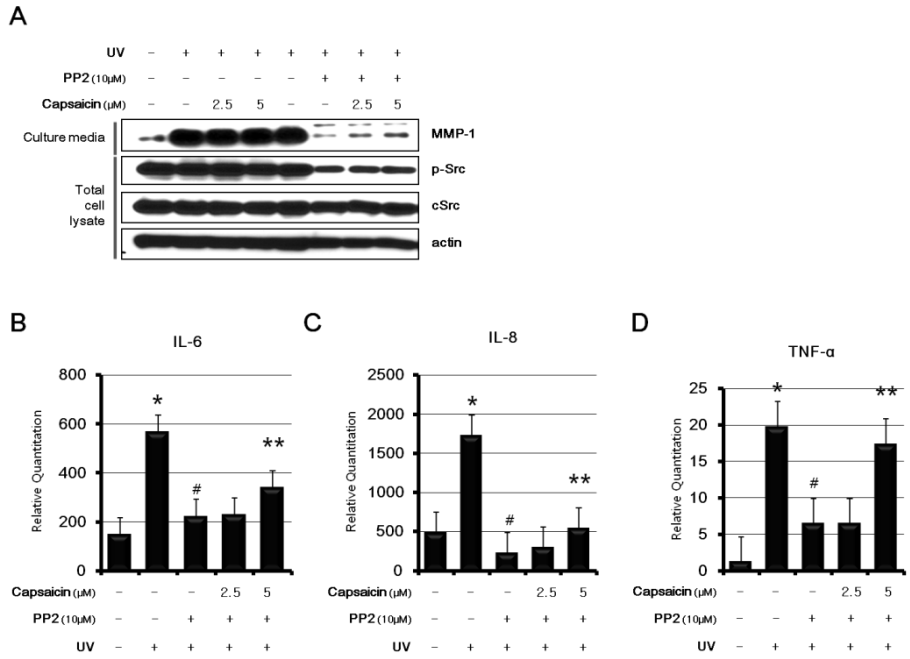

Figure 3. Inhibitory effect of PP2 on UV-induced responses is partially recovered by treatment with TRPV1 agonist.

HaCaT cells were cultured in 60 mm dish. Culture media was changed with serum-free media and incubated for 24 hours. After pretreatment with a TRPV1 agonist, capsaicin, and the specific Src inhibitor, PP2, for 30 minutes, the cultured HaCaT cells were treated with UV-irradiation (75 mJ/cm^2). Fresh media containing capsaicin and PP2 was added, and the cells were further incubated for 48 hours. The amounts of MMP-1 released into the culture media and phospho-Src, and total-Src protein from total cell lysates were determined by Western blotting (Fig. 3A).

The protein levels of IL-6, IL-8, and TNF-α were analyzed by ELISA (Fig. 3B, 3C, 3D). Results were expressed as mean values ± SE. *P < 0.05 versus UV-untreated control group. $^{\#}$P < 0.05 versus UV-treated group. **P < 0.05 versus UV-treated and PP2-treated control group.

UV induces TRPV1 trafficking into cell membrane.

To investigate whether TRPV1 moves into cell membrane from cell cytosol by UV-irradiation, TRPV1 trafficking was observed by staining with anti-TRPV1 antibody in HaCaT cells. The cultured HaCaT cells were treated with UV-irradiation (75 mJ/cm^2), and then cells were fixed and stained for TRPV1 (green) using anti-TRPV1 antibody at indicated time after UV treatment (at 0, 5, 15 minutes after UV treatment, Fig. 4). Indeed, TRPV1 moved into cell membrane from 0 to 15 minutes after UV treatment (indicated yellow arrow, The data shown are representative of three independent experiments, Fig. 4).

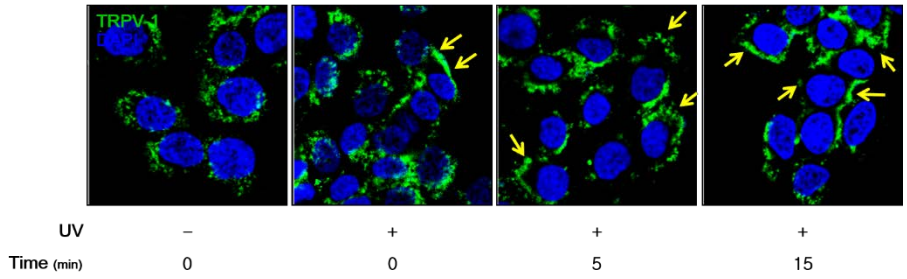

Figure 4. UV induces TRPV1 trafficking into cell membrane.

HaCaT cells were seeded on a chamber slide, and cultured for 24 hours in a humidified CO_2 incubator at 37°C. The cultured HaCaT cells were treated with UV-irradiation (75 mJ/cm^2). Cells were fixed with 4% paraformaldehyde and stained for TRPV1 (green) using anti-TRPV1 antibody at indicated time after UV treatment. Nuclei were counterstained with 4',6-diamidino-2-phenylindole (DAPI, blue). HaCaT cells were photographed with a Zeiss LSM 510 META confocal laser-scanning microscope (Zeiss, Yena, Germany).

UV-induced TRPV1 trafficking is inhibited by treatment with PP2

To investigate whether Src kinase regulates UV-induced TRPV1 trafficking, TRPV1 trafficking was observed by staining in HaCaT cells with PP2 treatment or not. The cultured HaCaT cells were pretreated with PP2 for 30 minutes, and then cells were treated with UV. HaCaT cells were fixed and stained for TRPV1 (green) using anti-TRPV1 antibody at indicated time after UV treatment (at 0, 5, 15 minutes after UV treatment). By pretreatment of PP2, TRPV1 did not move into cell membrane despite of UV-irradiation (at 5 minutes after UV treatment, representatively, indicated red arrow, Fig. 5A) (The data shown are representative of three independent experiments).

To compare cell membrane with other regions, HaCaT cells were stained with cell membrane specific protein, wheat germ agglutinin (WGA, green, Fig. 5B). By PP2 pretreatment, TRPV1 did not translocate into cell membrane at 5 minutes after UV treatment (red, Fig. 5B). HaCaT cells were photographed visualized using a Zeiss LSM 510 META confocal laser-scanning microscope (Zeiss, Yena, Germany) (The data shown are representative of three independent experiments).

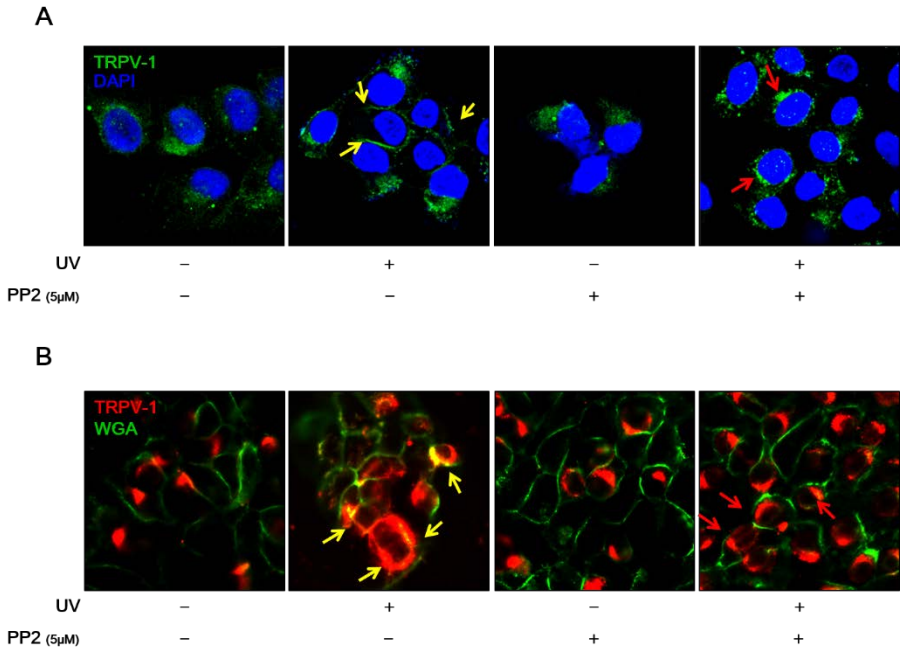

Figure 5. UV-induced TRPV1 trafficking is inhibited by treatment with PP2

HaCaT cells were seeded on a chamber slide, and cultured for 24 hours in a humidified CO_2 incubator at 37°C. After pretreatment with the specific Src inhibitor, PP2, for 30 minutes, the cultured HaCaT cells were treated with UV-irradiation (75 mJ/cm^2). Cells were fixed with 4% paraformaldehyde and stained for TRPV1 (green) using anti-TRPV1 antibody at indicated time after UV treatment. Nuclei were counterstained with 4',6-diamidino-2-phenylindole (DAPI, blue).

To distinguish cell membrane from other regions, HaCaT cells were stained with a cell membrane specific protein, wheat germ agglutinin (WGA, green, Fig. 5B) and TRPV1 was immunostained with anti-TRPV1 antibody (red, Fig. 5B) at indicated time after UV treatment. HaCaT cells were visualized with a Zeiss LSM 510 META confocal laser-scanning microscope (Zeiss, Yena, Germany).

UV-induced TRPV1 trafficking is mediated by Src.

To determine the co-localization of TRPV1 with Src after UV-irradiation, both TRPV1 and Src proteins were observed by confocal microscopy visualized. HaCaT cells were stained for TRPV1 (green, Fig. 6A) and Src (red) using anti-TRPV1 antibody and anti-Src antibody at 5 minutes after UV exposure. After UV-irradiation, both TRPV1 and Src kinase simultaneously moved into the cell membrane at 0 to 5 minutes (yellow arrow, Fig. 6A). However, at 15 minutes after UV-irradiation, TRPV1 was separated from Src kinase. (The data shown are representative of three independent experiments).

This UV-induced co-localization of TRPV1 and Src kinase was inhibited by PP2 treatment. In HaCaT cells with PP2 pretreatment, UV failed to induce the trafficking of TRPV1 and Src into the cell membrane (Fig. 6B).

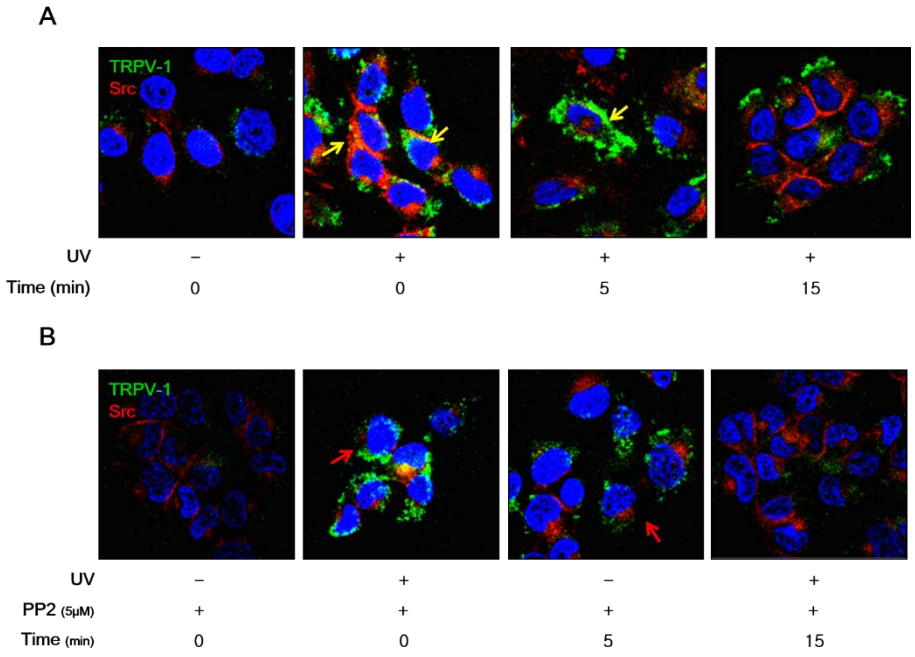

Figure 6. UV-induced TRPV1 trafficking is mediated by Src.

To compare the co-localization of TRPV1 with Src after UV-irradiation, HaCaT cells were seeded on a chamber slide, and cultured for 24 hours in a humidified CO_2 incubator at 37°C. The cultured HaCaT cells were treated with UV-irradiation (75 mJ/cm^2). Cells were fixed with 4% paraformaldehyde and stained for TRPV1 (green, 6A, 6B) and Src (red, 6A, 6B) using anti-TRPV1 antibody and anti-Src antibody at 0 to 15 minutes after UV treatment. Nuclei were counterstained with 4',6-diamidino-2-phenylindole (DAPI, blue, 6A, 6B). HaCaT cells were

photographed with a Zeiss LSM 510 META confocal laser-scanning microscope (Zeiss, Yena, Germany).

A model of the UV-induced TRPV1 trafficking mediated by Src and the downstream signaling pathways

These results suggest that UV induces TRPV1 trafficking into cell membrane from the vesicle in cell cytosol. Although it is remained to solve, Src tyrosine kinase may bind to TRPV1 and phosphorylate the tyrosine residue of TRPV1, which leads to the trafficking of TRPV1 into cell membrane. And TRPV1 localized in cell membrane could be activated by the activators including PKC and CaMKII, which causes conformational change of TRPV1 and open the channel. The calcium influx through TRPV1 mediates the downstream signaling pathway of UV-induced responses including the increase of MMPs and pro-inflammatory cytokines expression, which result in skin aging.

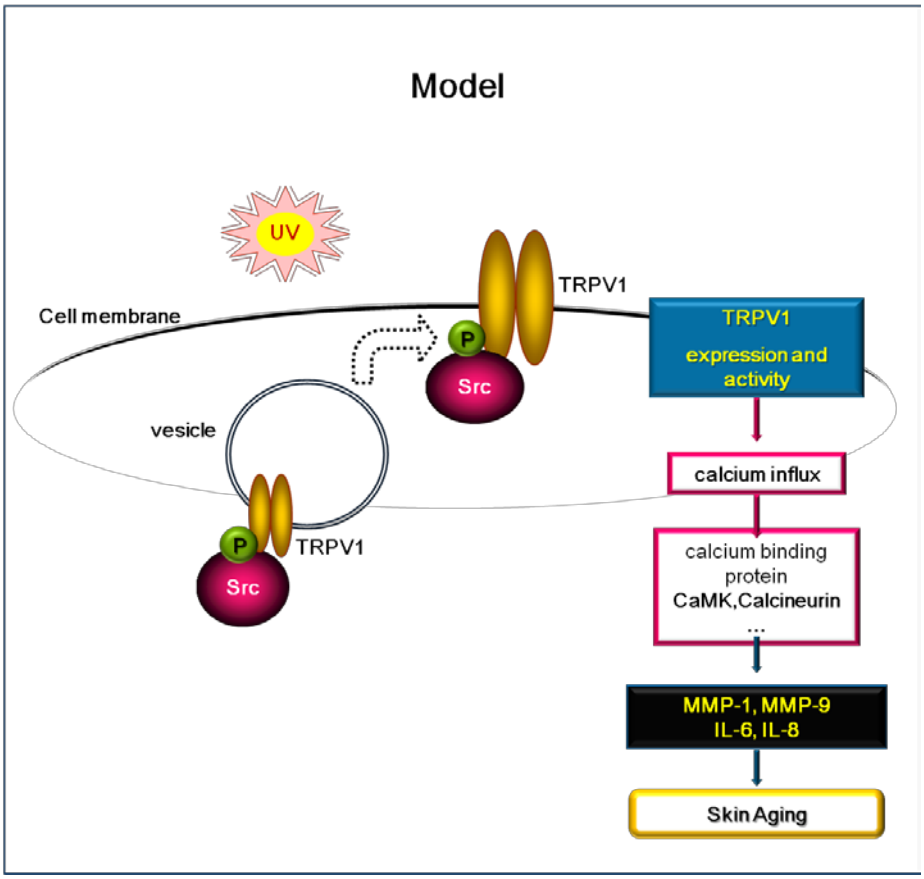

Figure 7. A model of the UV-induced TRPV1 trafficking mediated by Src and the downstream signaling pathways

UV radiation induces the trafficking of TRPV1 into the cell membrane through Src kinase. This initial activation step of TRPV1 by UV radiation leads to the downstream signaling associated with UV-induced MMP-1 or pro-inflammatory cytokine expression, which is mediated by calcium influx through TRPV1 translocalized into cell membrane.

DISCUSSION

Recently, as increasing exposure to harmful UV radiation have become a significant problem to human society due to the destruction of ozone layer, the interest of UV response on the nature and underlying mechanisms of UV responses has been expanding exponentially. UV response was suggested to be attributed to a damaged DNA or a by-product of DNA damage [8, 11], and many UV-inducible genes or the transcription factors including AP-1 or NF-κB regulating UV induction responses have been proposed [109-111]. Over the past decades, studies on the mechanism of signal transduction following UV radiation have been reported, and according to the previous study, Src tyrosine kinase is activated as the earliest step of UV-induced responses, followed by activation of Ha-Ras and Raf-1. Since Src and Ras are generally associated with the inner face of the cellular membrane and participate in downstream signaling pathway from cell surface receptors, it has been suggested that the UV response is initiated at the cell surface membrane rather than within the nucleus [112-114]. In this study, I demonstrated that UV-induced TRPV1 trafficking into cell surface membrane is mediated by Src tyrosine kinase. These results support that the UV signal transduction occurs at the cell surface membrane. I also showed that blocking Src tyrosine kinase with Src specific inhibitor, PP2, could significantly inhibit UV-induced MMP-1 and pro-inflammatory cytokine

expression. These results imply that Src tyrosine kinase acts as an important role in signal transduction during UV-induced skin aging process. And because this inhibitory effect by Src inhibitor was attenuated by capsaicin, a TRPV1 agonist, I suggest it could be inferred that TRPV1 is a downstream signaling molecule regulated by Src tyrosine kinase. Therefore, both Src tyrosine kinase and TRPV1 have important role in the UV-induced responses at the surface membrane. Subsequently, at the surface membrane, other kinases including PKC and CaMKII could phosphorylate and activate the TRPV1 ion channel, leading to conformational change of TRPV1 and inducing calcium influx through TRPV1.

It has been well described that TRPV1 plays a role in heat or UV-induced responses [35-38]. Since TRPV1 can be activated when it is localized at the cell surface membrane, it has to be trafficked by certain mediators [63]. And this trafficking process provokes the downstream signaling more rapidly. And this preconditioning step for the further sensitization to the noxious stimuli such as heat is a well-known mechanism for TRPV1 activation [79, 115]. In this study, I showed that UV induced TRPV1 trafficking into cell surface membrane. The results reported here imply that by not only heat, but also UV stimulus, the nociceptor TRPV1 could be trafficked and sensitized for further activation.

Tyrosine phosphorylation has been suggested to regulate the trafficking

of ion channels, transporters and receptors [74, 76]. In particular, a recent study demonstrated that phosphorylation of a single tyrosine residue, Y200, in TRPV1 by Src is the major mechanism leading to NGF-induced rapid sensitization of TRPV1. Therefore, it remains to be solved that UV-induced TRPV1 trafficking, which is thought to be mediated by Src, requires the phosphorylation of Y200 in TRPV1, and this tyrosine phosphorylation is necessary for serine or threonine phosphorylation in TRPV1 by PKC or CaMKII.

In this study, I found that Src kinase has a critical role in UV-induced TRPV1 trafficking and activation. However, since the molecular mechanism about the initial activation of TRPV1 by UV radiation is still not clearly established, investigation of this mechanism in detail should be further studied.

Chapter II.

A synthetic peptide targeting TRPV1 inhibits UV-induced responses in HaCaT cells and in mouse skin.

ABSTRACT

Transient receptor potential vanilloid 1 (TRPV1) channel can be activated by vanilloids, exposure to ultraviolet (UV) light, heat, or protons, and conditions that occur during tissue injury. In the present study, I designed a new TRPV1 inhibitory peptide (TIP) mimicking the specific site in TRPV1, phosphorylated by both protein kinase C (PKC) and Ca^{2+}/calmodulin-dependent protein kinase (CaMKII) in TRPV1 (a.a 701-709 : QRAITILDT), and investigated whether this TIP can ameliorate UV-induced responses.

Treatment with this TIP prevented UV-induced mRNA and protein expression of MMP-1 and pro-inflammatory cytokines such as IL-6 and TNF-α in HaCaT cells. Moreover, this peptide reduced heat-induced MMP-1 expression in HaCaT cells. Treatment with this peptide also inhibited capsaicin-induced calcium influx in HaCaT cells.

TIP prevented UV-induced skin thickening. The mRNA and protein level of UV-induced MMP-13 tended to be reduced by this peptide. The UV-induced MMP-9 increase was also inhibited. Additionally, TIP prevented UV-induced apoptosis in the skin of hairless mice. In conclusion, I demonstrated that a novel synthetic peptide targeting TRPV1 could inhibit UV-induced MMPs or pro-inflammatory cytokines expressions in HaCaT cells and mice skin.

Keywords: TRPV1 inhibitory peptide (TIP), UV, MMPs, pro-inflammatory cytokines, mice skin

MATERIALS AND METHODS

Materials

TRPV1 inhibitory peptide (TIP, QRAITILDT), palmitoyl-linked TRPV1 inhibitory peptide (PA-TIP), and control peptide (composed with each of contrary amino acid sequences, ILTQRRTIA) were producd in Peptron. Co. (Daejeon, Korea) (Fig. 1). The calcium-sensitive indicator, Fluo-4 AM, was obtained from Molecular Probes (Carlsbad, CA). Capsaicin (M2028) was purchased from Sigma Aldrich (St. Louis, MO). Anti-human MMP-1 antibody was acquired from Lab Frontier (Seoul, Korea). Goat polyclonal antibody against actin (sc-1616) was supplied by Santa Cruz Biotechnology (Santa Cruz, CA). Rabbit polyclonal antibody against MMP-13 (ab39012) was supplied by abcam (Cambridge, UK). The cell culture media, antibiotics, and Trizol reagent were purchased from Life Technologies (Rockville, MD). Fetal bovine serum (FBS) was obtained from Hyclone (Logan, UT).

Methods

1. Cell culture and treatments

The immortalized human keratinocytes cell line, HaCaT, was cultured in Dulbecco's modified Eagle's media (DMEM) supplemented with glutamine (2 mM), penicillin (400 U/ml), streptomycin (50 mg/ml), and 10% FBS at 37°C in a humidified atmosphere containing 5% CO_2. For treatment, the cells were cultured to 80% confluence and then maintained in culture media without FBS for 24 hours. The cells were washed with phosphate buffered saline (PBS) and irradiated with UV. After UV treatment, the culture medium was replaced with fresh medium without FBS, and the cells were further incubated for 48 hours. TRPV1 inhibitory peptide (TIP) was added at 30 minutes before UV treatment, and incubated for 48 hours after UV treatment.

2. UV-irradiation

In the Western blot and real-time RT-PCR experiment, the HaCaT cells were irradiated with a Philips TL 20W/12 RS fluorescent sun lamp with an emission spectrum ranging between 275 and 380 nm (peak, 310–315 nm) [116, 117]. A Kodacel filter (TA401/407; Kodak) was used to block UVC, which has wavelengths of < 290 nm. The UV strength was measured using a Waldmann UV meter (model 585100).

For UV exposure to animal, F75/85W/UV21 fluorescent sunlamps with an emission spectrum between 275 and 380 nm (peak at 310–315 nm)

served as the UV source [116, 117]. A Kodacel filter (TA401/407; Kodak, Rochester, NY) was mounted 2 cm in front of the UV tube for removal of wavelengths < 290 nm (UVC). Irradiation intensity at the skin surface was measured using a UV meter (model 585100; Waldmann Co., Villingen-Schwenningen, Germany). The irradiation intensity 30 cm from the light source was 1.0 mW/cm^2. We initially measured the minimal erythema dose (MED) on the dorsal skin of mice. MED is defined as the minimum amount of radiation required to produce an erythema with sharp margins after 24 hours. UV was exposed to the dorsal skin of hairless mice in 2MED (1MED = 100 mJ/cm^2).

For UV-irradiation to human, human buttock skin was irradiated with a Waldmann UV-800 (Waldmann, Villingen-Schwenningen, Germany) phototherapy device and a F75/85W/UV21 fluorescent lamp with an emission spectrum between 285 and 350 nm (peak, 310−315 nm), as described previously (Seo et al., 2001). The strength of UV-irradiation at the skin surface was measured using a Waldmann UV meter (model 585100). The buttock skin was irradiated with UV light filtered through a Kodacel filter (TA401/ 407; Kodak, Rochester, NY), and the minimal erythema dose (MED) was determined at 24 hours before irradiation. The MED usually ranges between 70 and 90 mJ/cm^2 for the brown skin of Koreans. In this study, I used 2 MED. The irradiated and non-irradiated buttock skin samples were obtained from each subject using a

punch biopsy. This study was approved by the Institutional Review Board at the Seoul National University Hospital, and all subjects provided written informed consent.

3. Heat shock treatment

For heat treatment, cells were cultured to 80% confluence and then maintained on culture media without FBS for 24 hours. The culture dishes were sealed with parafilm and immersed for 30 minutes into a circulating water bath thermo-regulated at 37 ± 0.05°C for the control treatment or at 44 ± 0.05°C for the heat shock treatment. After heat treatment, culture media were replaced with fresh media without FBS and the cells were further incubated for the indicated times. TRPV1 inhibitory peptide (TIP) or control peptide (CNT-peptide) was added at 30 minutes before the control or heat shock treatment.

4. Western blot analysis

In order to determine the amounts of MMP-1 secreted into the culture media from HaCaT cells, equal aliquots of conditioned culture media from an equal number of cells were fractionated by 10% SDS–PAGE, transferred to a Hybond ECL membrane (Amersham Biosciences,

Buckinghamshire, England), and analyzed by Western blotting with a anti-human MMP-1 antibody (Lab Frontier) by enhanced chemiluminescence (Amersham Biosciences). As controls, the levels of the corresponding β-actin were determined in the same cell lysates using the antibodies for β-actin (Santa Cruz Biotechnology). The signal strengths were quantified using a densitometric program (TINA; Raytest Isotopenme b gerate, Straubenhardt, Germany).

In order to measure MMP-13 protein level in animal, skin tissues were homogenized in ice-cold lysis buffer [50 mM Tris–HCl, pH 7.4, 150 mM NaCl, 2 mM ethylenediamine tetraacetic acid (EDTA), 5 mM phenylmethanesulfonyl fluoride (PMSF), and 1 mM dithiothreitol (DTT), 1% Triton X-100] with freshly added protease inhibitor cocktail (Roche, Indianapolis, IN). Homogenates were then centrifuged at 15,000g for 30 minutes at 4°C, and supernatants were then collected and stored at -70°C. Protein contents in lysates were determined using the Bradford assay. Equal amounts of protein were resolved over 8–16% Tris–Glycine SDS-PAGE gels, and then electrophoretically transferred to PVDF membranes. Blots were subsequently blocked with blocking buffer (5% nonfat dry milk, 1% Tween-20; in 20 mM TBS, pH 7.6) for overnight at 4°C and incubated rabbit polyclonal antibody against MMP-13 (ABCAM).

In order to measure MMP-1 protein level in human skin, after skin samples were obtained from each subject by punch biopsy, the samples were incubated at 58°C for 2 minutes in phosphate-buffered saline (PBS). To analyze the expression of MMP-1, skin samples were homogenized and extracted with lysis buffer containing 50 mm Tris–HCl (pH 7.4), 1% Triton X-100, 150 mm NaCl, 1 mM EDTA, 1 mM EGTA, 10 μg/ml aprotinin, 10 μg/ml leupeptin, 5 mm phenylmethylsulphonyl fluoride and 1 mM dithiothreitol. The protein content was determined using Bradford reagent (Bio-Rad, Hercules, CA, USA). Equal amounts (40 μg) of the protein samples were fractionated, transferred and analyzed by Western blotting using a anti-human MMP-1 antibody (Lab Frontier). As a control, the corresponding β-actin levels were determined in the same cell lysates using the antibodies for β-actin (Santa Cruz Biotechnology, SantaCruz, CA, USA). The signal strengths were quantified using a densitometric program (TINA; Raytest Isotopengemessgeraete GmbH, Straubenhardt, Germany).

5. Quantitative real-time RT-PCR

In order to measure mRNA of MMP-1, IL-6, and TNF-α in cells, total RNA was prepared from HaCaT cells using the Trizol method according to the manufacturer's protocol (Life Technologies). The isolated RNA

samples were electrophoresed in 1% agarose gels to assess the quality and quantity. One microgram of the total RNA was used in a 20 μL reaction volume for first-strand cDNA synthesis using a first-strand cDNA synthesis kit for RT-PCR, according to the manufacturer's instructions (MBI Fermentas, Vilnius, Lithuania). A quantitative real-time reverse transcription polymerase chain reaction (RT-PCR) was performed using 1 μg of the first-strand cDNA product and each primer pair (Table. 1) for the human genes: 36B4 (cDNA for human acidic ribosomal phosphoprotein PO), which did not change with UV or heat irradiation (Cho et al., 2008), MMP-1, IL-6, and TNF-α with an ABI PRISM 7500 Sequence Detection System (Applied Biosystems, Foster City, CA). The technique is based on the ability to detect the RT-PCR product directly with no downstream processing. This was accomplished by monitoring the increase in fluorescence of a dye-labeled DNA probe specific for each factor under study, plus a probe specific for the 36B4 gene, which is used as an endogenous control for the assay. The PCR reaction was carried out according to the manufacturer's instructions. As a negative control, the PCR reactions without the template cDNA were added to the reaction wells. All the samples were run in triplicate.

In order to measure mRNA level of MMP-13 and MMP-9 in animal, total RNA was prepared from whole skin tissue using Trizol reagent, according to the manufacturer's protocol (Life Technologies, Rockville,

MD). In order to assess quality and quantity, isolated RNA samples were electrophoresed in 1% agarose gels. One microgram of total RNA was used in a 20 μL first-strand cDNA synthesis reaction using a first-strand cDNA synthesis kit for quantitative real-time RT-PCR, according to the manufacturer's instructions (MBI Fermentas, Vilnius, Lithuania). For quantitative estimation of mRNA expression, PCR was performed on a 7500 Real-time PCR System (Applied Biosystems, Foster City, CA) using the SYBR Premix Ex TaqTM (Takara Bio Inc., Shiga, Japan), according to the manufacturer's instructions. Primers used were indicated in Table 1. PCR conditions were 50°C for 2 minutes, 95°C for 2 minutes, followed by 40 cycles at 95°C for 15 s and 60°C for 1 minutes. Data were analyzed using the 2-ΔΔCT method [118-120]; data were presented as the fold in gene expression normalized to 36B4 and relative to UV-irradiated or control cells. These experiments were performed in triplicate and independently repeated at least three times.

In order to measure mRNA of MMP-1 and IL-1β in human, skin samples were obtained from each subject by punch biopsy, the samples were incubated at 58°C for 2 minutes in PBS. Total RNA was prepared from skin tissue using Trizol reagent according to the manufacturer's protocol (Life Technologies, Rockville, MD, USA). The isolated RNA samples were electrophoresed in 1% agarose gels to assess the quality and quantity. One microgram of total RNA was used in a 20-μL first-strand cDNA

synthesis reaction using a first-strand cDNA synthesis kit for RT-PCR according to the manufacturer's instructions (MBI Fermentas, Vilnius, Lithuania). For quantitative estimation of mRNA expression, PCR was performed on a 7500 Real-time PCR System (Applied Biosystems, Foster City, CA) using the SYBR Premix Ex TaqTM (Takara Bio Inc., Shiga, Japan), according to the manufacturer's instructions. Primers used were indicated in Table 1. PCR conditions were 50°C for 2 minutes, 95°C for 2 minutes, followed by 40 cycles at 95°C for 15 seconds and 60°C for 1 minutes. Data were analyzed using the 2-ΔΔCT method [118-120]; data were presented as the fold in gene expression normalized to 36B4 and relative to UV-irradiated or control cells. These experiments were performed in triplicate and independently repeated at least three times.

6. Ca^{2+}-imaging experiments

HaCaT cells were cultured on cover glasses, then loaded with 4 mM Fluo-4 AM (Molecular Probes) in serum-free medium at room temperature for 45 minutes. After washing three times with serum-free medium, cells on the cover glasses were transferred to custom-built observation chambers, and allowed to accommodate for 20 minutes. Capsaicin was used at a final concentration of 1 mM in Tyrode's buffer (140 mM NaCl, 5 mM KCl, 1 mM $MgCl_2$, 2 mM $CaCl_2$, 10 mM glucose, and 10 mM HEPES [pH

7.2]). The fluorescence intensity was measured using a confocal laser scanning microscope (LSM 510 META, Zeiss) fitted with appropriate filters and a PL Fluotar objective (200x0.5 NA) that was controlled by SCAN Ware 5.10 software (Zeiss). The experiments were performed at 37°C in a humidified chamber. The measurements lasted for 200 seconds, with images taken every 1 or 4 seconds.

7. Immunofluorescence

For immunofluorescence staining, the HaCaT cells were seeded in 4-well chamber slides (Falcon, BD Biosciences, Bedford, MA) with 1.5 x 10^4 cells per well and incubated for 24 hours. FITC-linked TIP was treated for 30 minutes, while the negative control group was treated with serum-free media containing TIP. Cells were fixed in 4% paraformaldehyde in phosphate-buffered saline (PBS) for 30 minutes. Fixed cells were blocked with blocking solution (10% goat serum, 0.5% gelatin and 0.1% Triton X-100 in PBS) for 30 minutes. The negative control (NC) was incubated with goat anti-rabbit IgG. Both FITC-linked TIP and primary antibody treated cells were washed 3 times with PBS and then incubated with fluorescein-conjugated secondary antibodies (Alexa Fluor®) diluted in blocking solution for 1 hour. Subsequently, the coverslips were mounted onto slides after the treatment of mounting solution with DAPI. Cells

were observed under the fluorescence microscope (Carl Zeiss, Jena, Germany). Specimens were visualized with 405, 488, 545 nm lasers.

8. Animals and Treatment of peptide and UV

Six-week-old female albino hairless mice (Skh-1) were obtained from Bio Genomics, Inc. (Seoul, Korea). Animals were acclimated for 1 week prior to the study and had free access to food and water. All experimental protocols were approved by the Committee for Animal Care and Use at Seoul National University.

Animals were divided into four groups in each group of i - iv as follows: (i) UV unexposed and vehicle treated mice, (ii) UV unexposed and 1 mM TRPV1 inhibitory peptide treated mice (iii) UV-irradiated and vehicle treated mice (iv) UV-irradiated and 1 mM TRPV1 inhibitory peptide treated mice. Vehicle was composed of ethanol (30%) and polyethylene glycol (70%). Vehicle and TRPV1 inhibitory peptide were applied to the dorsal skin surface at 0 and 24 hours after UV-irradiation. These mice were sacrificed at 48 hours after UV-irradiation and skin specimens were biopsied.

9. Skin fold thickness measurement

Using a caliper (PEACOCK, Ozaki MFG Co. Ltd., Tokyo, Japan), skin fold thickness was measured at 24 hours before UV-irradiation and 48 hours after UV-irradiation. Midline skin was manually pinched upward at the neck and at the base of the tail, and skin fold thickness was then measured mid-way between the neck and hips.

10. Hematoxylin and eosin (H&E) staining and skin thickness measurements

Mouse skin samples were fixed in 10% buffered formalin for 24 hours, and embedded in paraffin. Serial sections (4 μm) were mounted onto silane-coated slides, and stained with hematoxylin solutions for nuclear staining and eosin solutions for cytoplasm (H&E) by routine methods as previously described [29]. Epidermal and dermal thickness was measured using an image analysis program (BMI plus software, BumMi Universe Co., Kyungki, Korea).

11. Terminal dUTP nick-end labelling analysis

Terminal dUTP nick-end labelling was performed using a commercial kit (ApopTag Plus Peroxidase *In Situ* Apoptosis Detection Kit; Chemicon International, Temecula, CA, USA). Skin samples from animal were cut

into sections of 4 μm thickness and fixed in acetone for 5 min at -20 °C. The sections were blocked in 3% hydrogen peroxide for 5 min at room temperature. The sections were incubated with the equilibration buffer (10 seconds at room temperature), and the working-strength TdT enzyme in a humidified chamber (1 h at 37°C), followed by incubation with the stop/wash buffer (10 min at room temperature). Sections were incubated with the antidigoxigenin peroxidase conjugate (30 min at room temperature). The colour reaction was developed using the AEC substrate system (Zymed).

12. Human skin sample and UV or TIP treatment

Adult Korean male volunteers (more than the age of 30 years, n=8) without current or prior skin disease provided skin samples. Either 6-mm punch biopsy specimens were obtained from buttock skin.

The regions were divided into four groups in each group of i - iv as follows: (i) UV unexposed and vehicle treated region, (ii) UV-irradiated and vehicle treated region (iii) UV-irradiated and 1mM TRPV1 inhibitory peptide (TIP) treated region (iv) UV-irradiated and 1mM palmitoyl-TRPV1 inhibitory peptide (PA-TIP) treated region. Vehicle was composed of ethanol (30%) and polyethylene glycol (70%).

The buttock skin was irradiated with a Waldmann UV-800 (Waldmann, Villingen-Schwenningen, Germany) phototherapy device and a F75 /85W/UV21 fluorescent lamp with an emission spectrum between 285 and 350 nm (peak at 310–315 nm), as described previously [121]. The strength of UV-irradiation at the skin surface was measured using a Waldmann UV meter (model 585100). The buttock skin was irradiated with UV light filtered through a Kodacel filter (TA401 / 407; Kodak, Rochester, NY, USA), and the MED (minimal erythema dose) was determined 24 hours after irradiation. The MED usually ranged between 70 and 90 mJ /cm^2 for the brown skin of Koreans. This study used 2MED (between 140 and 180 mJ/cm^2). After UV-irradiation, 25 μL of vehicle, TRPV1 inhibitory peptide (TIP, 1 mM), or palmytoyl acid-linked TRPV1 inhibitory peptide (PA-TIP, 1 mM) was applied to each region on the buttock skin. Irradiated and non-irradiated or TIP treated or non-treated buttock skin samples were obtained from each subject using a punch biopsy. This study was approved by the Institutional Review Board at the Seoul National University Hospital, and all subjects provided written informed consent.

Table 1. Primer sequences for human and mouse genes for quantitative real-time PCR.

Human gene	5' primer sequence	3' primer sequence
h36B4	TCG ACA ATG GCA GCA TCT AC	TGA TGC AAC AGT TGG GTA GC
hMMP-1	ATT CTA CTG ATA TCG GGG CTT TGA	ATG TCC TTG GGG TAT CCG TGT AG
hIL-1β	CTG TCC TGC GTG TTG AAA GA	TTC TGC TTG AGA GGT GCT GA
hIL-6	GCA GAT GAG TAC AAA AGT CC	GCA GAA TGA GAT GAG TTG TC
hTNF-α	TCC TTC AGA CAC CCT CAA CC	AGG CCC CAG TTT GAA TTC TT
Mouse	**5' primer sequence**	**3' primer sequence**
m36B4	TGG GCT CCA AGC AGA TGC	GGC TTC GCT GGC TCC CAC
mMMP-13	CAT CCA TCC CGT GAC CTT AT	GCA TGA CTC TCA CAA TGC GA
mMMP-9	TTG AGT CCG GCA GAC AAT CC	CCT TAT CCA CGC GAA TGA CG

RESULTS

TIP as a competitive inhibitory substance of TRPV1 targeting Thr 705.

For inhibition of TRPV1 activity, since the single amino acid residue Thr 705 residue on TRPV1 is phosphorylated by PKC and CaMKII, followed by conformational change and gate-open of TRPV1 channel. I synthesized a 9-amino acid-peptide mimicking this region including Thr 705, 701-709 residues for a competitive inhibition as a strategy to block this site (Fig. 1)

Activation of Ca^{2+} influx by capsaicin is inhibited by treatment with TIP

To confirm the effect of TIP in HaCaT cells, the capsaicin-induced increase in intracellular Ca^{2+} concentration ($[Ca^{2+}]_i$) was measured. The fluorescence intensity of Fluo-4 (F_{fluo4}) was increased by capsaicin (Fig. 8A). 1 mM of capsaicin increased the F_{fluo4} to 217.0±9.7% of control values (The data shown were measured from 11 different cells marked as different regions of interest, Fig. 8B). Pretreatment with TIP (10 μM) inhibited the capsaicin-induced increase of $[Ca^{2+}]_i$ (126.6±6.3% of control values) (The data shown were measured from 11 different cells marked as different regions of interest, Fig. 8B).

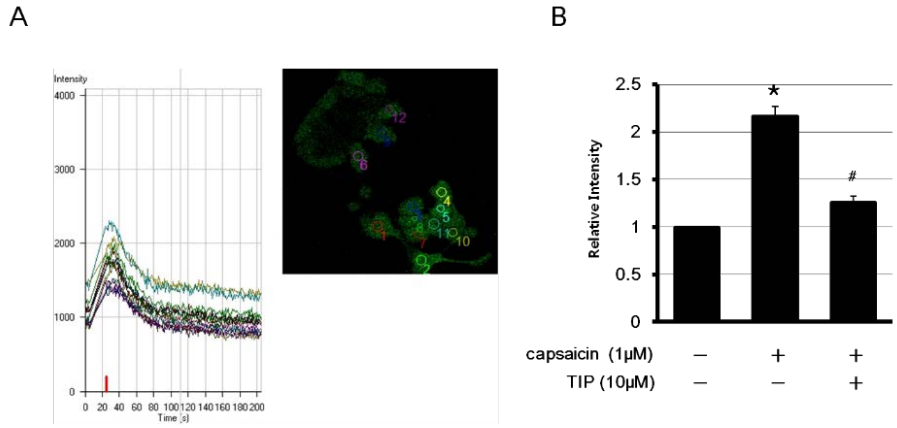

Figure 8. TIP inhibits capsaicin-induced Ca^{2+} influx in HaCaT cells.

HaCaT cells were cultured on cover glasses, then loaded with 4 mM Fluo-4 AM (Molecular Probes) in serum-free medium at room temperature for 45 minutes. Tyrode's buffer containing 1 mM capsaicin was loaded in dish. The fluorescence intensity was measured as described in Method. Fluorescence signals of Fluo-4 loaded for monitoring $[Ca^{2+}]_i$ were observed from 0 to 200 seconds after treatment with capsaicin from 11 different cells marked as different regions of interest. Results are expressed as mean values ± SE. ($^{*}P < 0.05$ versus control group; $^{\#}P < 0.05$ versus capsaicin-treated group.) The relative intensity ratio of calcium influx is measured at about 20 seconds after capsaicin treatment (indicated red bar, Fig. 8A, 8B).

TIP inhibits UV-induced MMP-1 expression

I investigated whether the UV-induced MMP-1 expression was affected by treatment with TIP. For this purpose, HaCaT cells were exposed to UV (75 mJ/cm^2), and the level of secreted MMP-1 was measured in culture media 48 hours after UV-irradiation. Consistent with previous reports. UV-irradiation increased the level of MMP-1 protein expression. Pretreatment of HaCaT cells with TIP decreased the UV-induced MMP-1 expression compared with the control peptide-treated UV-irradiated group (Fig. 9). UV-irradiation increased the level of MMP-1 protein expression (158.6±12.1%, Fig. 9A). Pretreatment with TIP decreased the UV-induced MMP-1 protein expression compared with the UV-irradiated group (125.7±6.1%, 94.8±42.1%, 71.4±28.8% of the control group by 1, 5, and 10 μM, respectively; Fig. 9A) (The data shown are representative of three independent experiments). Quantitative RT-PCR analysis showed an increased MMP-1 mRNA at 48 hours after UV-irradiation (200.0±76.4% of the control group, Fig. 9B) (The data shown are representative of three independent experiments). TIP decreased the UV-induced MMP-1 mRNA expression compared with the control peptide-treated UV-irradiated group (88.2±31.1%, 76.1±22.1%, 82.4±16.6% of the control group by 1, 5, and 10 μM, respectively; Fig. 9B) (The data shown are representative of three independent experiments).

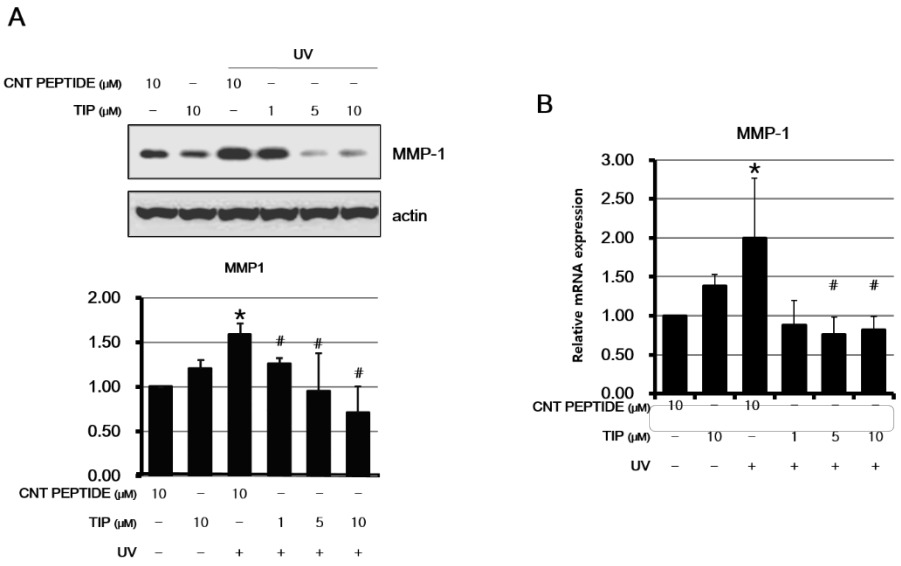

Figure 9. TIP inhibits UV-induced MMP-1 expression in HaCaT cells.

HaCaT cells were cultured in 60 mm dish. Culture media was changed with serum-free media and incubated for 24 hours. After pretreatment with TIP for 30 minutes, the cultured HaCaT cells were treated with UV-irradiation (75 mJ/cm^2). Fresh media containing control peptide (CNT peptide) or TIP were added, and the cells were further incubated for 48 hours. The amounts of MMP-1 protein released into the culture media were determined by Western blotting and quantified by densitometry. Each level of MMP-1 protein expression was normalized to that of the corresponding β-actin from total cell lysates, and the mean values are shown as bar graphs (Fig. 9A). The amounts of MMP-1 mRNA (Fig. 9B)

were analyzed at 48 hour post-treatment by quantitative RT-PCR (Fig. 9B). The mRNA expression level of MMP-1 was normalized versus that of the corresponding 36B4. Results are expressed as mean values ± SE. *P < 0.05 versus unirradiated control group. $^{\#}$P < 0.05 versus CNT peptide-treated UV-irradiated group.

TIP prevents UV-induced IL-6 and TNF-α expression

I also investigated the effects of TIP on UV-induced mRNA expression of the pro-inflammatory cytokines, IL-6 and TNF-α. UV-irradiation increased the level of IL-6 and TNF-α expression (700.6±89.4% and 289.2±34.3%, respectively; Fig. 10A, 10B). TIP decreased the UV-induced expressions of IL-6 and TNF-α mRNA respectively in HaCaT cells (465.1±110.6% and 193.5±5.4, respectively; Fig. 10A, 10B) (The data shown are representative of three independent experiments)..

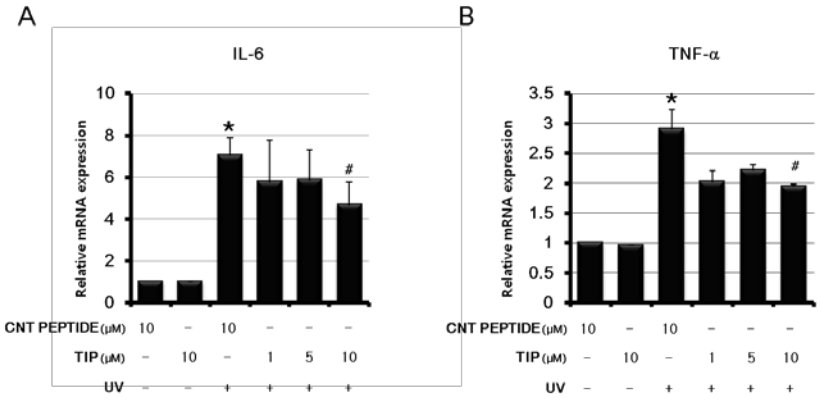

Figure 10. TIP inhibits UV-induced IL-6 and TNF-α expressions in HaCaT cells.

HaCaT cells were starved with serum-free media for 24 hours. After pretreatment with control peptide (CNT peptide) or TIP for 30 minutes, the cultured HaCaT cells were treated with UV-irradiation (75 mJ/cm^2). Fresh serum-free media containing signaling TIP were added, and the cells were further incubated for 48 hours. The mRNA level of pro-inflammatory cytokine such as IL-6 or TNF-α was determined by quantitative real-time RT-PCR. Each mRNA expression level of cytokine was normalized versus that of the corresponding 36B4. Results are expressed as mean values ± SE. $^*P < 0.05$ versus UV-untreated control group. $^{\#}P < 0.05$ versus UV-treated group.

Inhibition of TRPV1 suppresses heat-shock-induced MMP-1 expression in HaCaT cells

Because it is reported that TRPV1 signaling is involved in heat shock-induced MMP-1 expression [35, 36], I investigated whether TIP regulates heat-shock induced MMP-1 expression.

HaCaT cells were pretreated with TIP for 30 minutes, then the culture dishes were treated for 30 minutes in a water bath at 37°C (control) or at 44°C (heat shock) and MMP-1 release was determined 48 hours post-treatment. We observed that heat increased the protein level of MMP-1 (148.8±17.0% of the control group, Fig. 11A), and TIP significantly inhibited the heat-induced MMP-1 in a dose-dependent manner (138.9±23.4%, 81.9±18.9%, 15.8±7.6% of the control group by 1, 5, and 10 μM, respectively; Fig. 11A) (The data shown are representative of three independent experiments).

Quantitative RT-PCR analysis demonstrated an increase in MMP-1 mRNA at 48 hours after heat shock treatment (258.4±63.9% of the control group, Fig. 11B), which was also suppressed by 10 μM TIP treatment (190.9±55.2% of the control group, Fig. 11B) (The data shown are representative of three independent experiments).

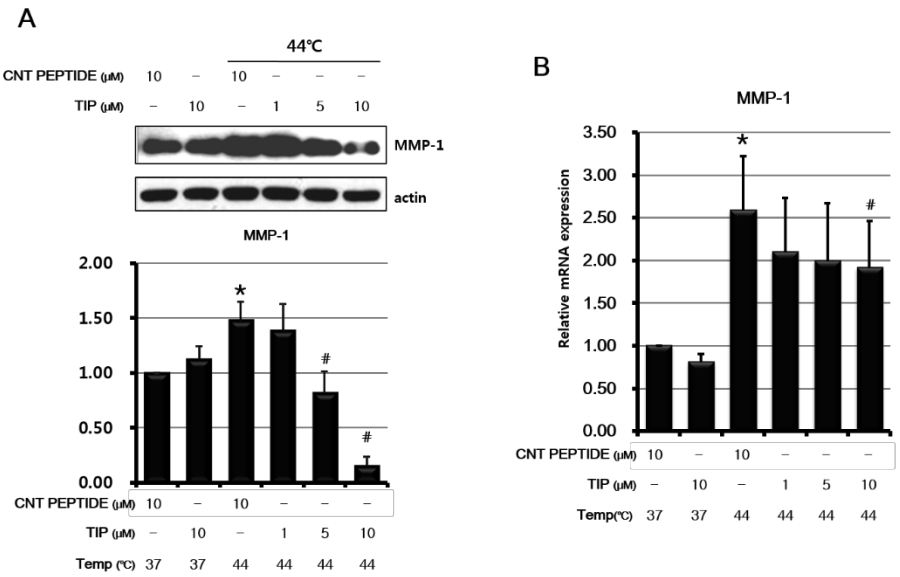

Figure 11. TIP inhibits heat-induced MMP-1 expression in HaCaT cells.

HaCaT cells were serum-starved for 24 hours. After being pretreated for 30 minutes with TIP, the cells were placed for 30 minutes in a water bath at 37 or 44°C. The cells were retreated with fresh media containing control peptide or TIP, and further incubated in a humidified CO_2 incubator at 37°C for 48 hours. The amounts of MMP-1 proteins released into cultured media (Fig. 11A) were analyzed at 48 hour post-treatment by Western blotting. Each level of MMP-1 protein was normalized to that of the corresponding β-actin. The amounts of MMP-1 mRNA (Fig. 11B) were analyzed at 48 hour post-treatment by quantitative real-time RT-PCR. Each level of MMP-1 mRNA was normalized versus that of the

corresponding 36B4 mRNA. Results are expressed as mean values ± SE.

*P < 0.05 versus 37°C control group. $^{\#}$P < 0.05 versus 44°C group.

Membrane permeability of TIP in HaCaT cells

Since the sequences of 701-709 of TRPV1 localize in a cytosol, TIP can play an inhibitory role to block the activation of TRPV1 when this peptide could enter into cytosol of cell. Therefore I investigated whether TIP can be influxed into cytosol of HaCaT cell without any stimulus.

To this purpose, an FITC-linked TIP was made and treated in HaCaT cells. I found that TIP could be influxed into cell membrane in a UV-independent manner (Fig. 12).

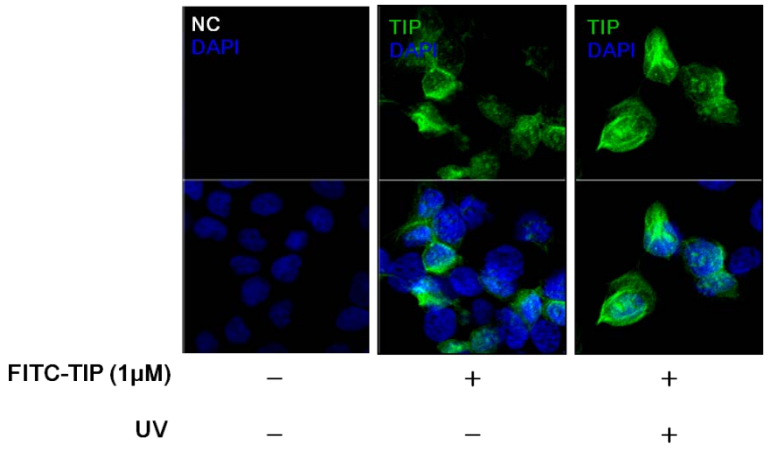

Figure 12. Membrane permeability of TIP in HaCaT cells

HaCaT cells were seeded on a chamber slide, and cultured for 24 hours in a humidified CO_2 incubator at 37°C. Then, cells were treated with serum-free media containing FITC-linked TIP (FITC-TIP, green) for 30 minutes, while the negative control group was treated with serum-free media containing TIP. After UV-irradiation (75 mJ/cm^2), cells were instantly fixed with 4% paraformaldehyde. The negative control (NC) was incubated with goat anti-rabbit IgG and then treated with Alexa 488 fluorescence antibody (green). Nuclei were counterstained with 4',6-diamidino-2-phenylindole (DAPI, blue). HaCaT cells were photographed with a Zeiss LSM 510 META confocal laser-scanning microscope (Zeiss, Yena, Germany) (The data shown are representative of three independent experiments).

TIP inhibites UV-induced skin thickening in hairless mice

UV exposure significantly increased skin thickness, as measured by a caliper, in hairless mice. UV-induced skin thickening was significantly inhibited in the 1 mM TIP-treated group compared with the UV-exposed group (79.0±9.8% of the control group, n=8, Fig. 13A).

I also confirmed the inhibitory effect of TIP on UV-induced skin thickening histologically in hematoxylin and eosin (H&E)-stained sections (Fig. 13B). UV-irradiation induced cutaneous inflammation in hairless mouse, which was alleviated by TIP post-treatment. Using an image analysis program, the epidermal or dermal thickness was measured in H&E-stained sections. UV exposure increased the epidermal thickness (UV-untreated control group: 15.22±0.64 μm, UV-treated group: 69.43±5.41 μm, n=8, Fig. 13C). TIP 1 mM treatment significantly inhibited UV-induced epidermal thickening, compared with the UV-exposed group (32.30±2.03 μm, n=8, Fig. 13C). Dermal thickening was significantly increased by UV-irradiation (UV-untreated control group: 133.94±5.61 μm, UV-treated group: 222.84±10.77μm, n=8, Fig. 13D), however; UV-induced dermal thickening was not decreased by TIP treatment (UV-treated and TIP treated: 236.04±5.47 μm, n=8, Fig. 13D).

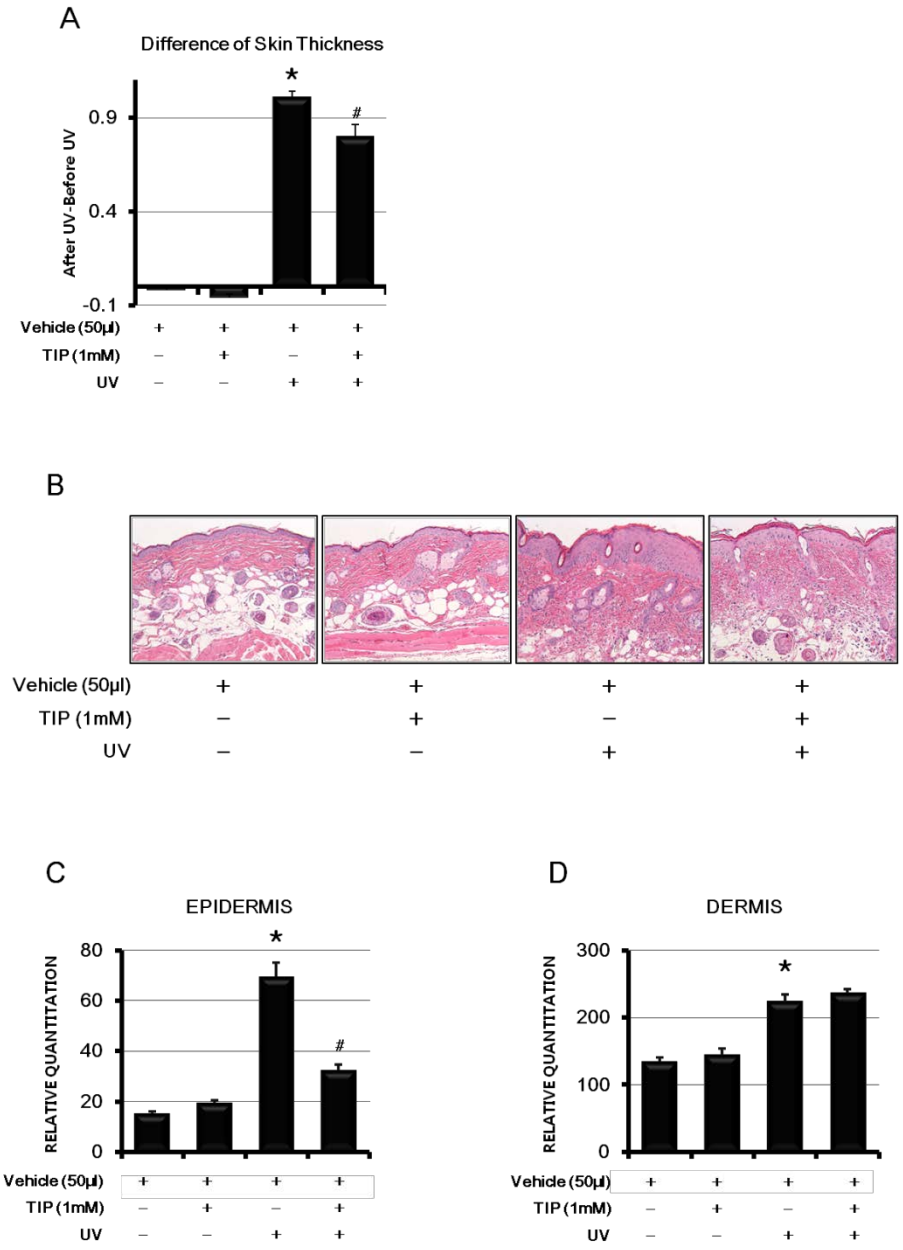

Figure 13. TIP attenuates UV-induced skin thickening.

Using a caliper, skin thicknesses were measured at midway between the neck and hips before and 48 hours after the single UV (200 mJ/cm^2)

treatment. TIP (50 μL of 1 mM) was applied to the dorsal skin of mice at 0 (immediately after UV) and 24 hours after single UV (200 mJ/cm^2) irradiation. These mice were biopsied at 48 hours after UV-irradiation. (Fig. 13A)

The below graph shows the relative difference of skin thickness between the values measured before and after UV-irradiation for each group, as mean values ± SE. Epidermal or dermal thicknesses are determined in H&E-stained sections (Fig. 13B). *P<0.05 versus non-exposed vehicle-treated control mice, $^{\#}$P<0.05 versus UV-exposed vehicle-treated mice (n = 8, Fig. 13C, 13D).

TIP inhibits UV-induced MMP expressions in hairless mice

To investigate the effects of TIP on UV-induced MMP expressions in hairless mice, I examined the protein and mRNA expression of MMP-13 (Fig. 14A, 14B), and also mRNA expression of MMP-9 (Fig. 14C).

I found that UV exposure significantly increased the expressions of MMP-13 protein and mRNA by Western blotting and quantitative real-time RT-PCR, respectively (Fig. 14A, 14B). UV-irradiation increased the level of MMP-13 protein expression (147.0±28.8% of the control group, n=8, Fig. 14A). Treatment of TIP decreased the UV-induced MMP-13 protein expression compared with the control group (91.6±12.9% of the control group, n=8, Fig. 14A). Furthermore TIP decreased the basal MMP-13 protein expression compared with the negative control group (52.7±13.2% of the control group, n=8, Fig. 14A).

Quantitative real-time RT-PCR analysis also showed that UV increased the mRNA level of MMP-13 (695.0±261.9% of the control group, n=8, Fig. 14B) and TIP decreased that of UV-induced MMP-13 (248.21±190.2% of the control group, n=8, Fig. 14B). And also 1 mM of TIP decreased the basal expression of MMP-13 mRNA compared with the UV-untreated control group (39.6±18.0%, n=8, Fig. 14B).

I also demonstrated that UV exposure significantly increased the expressions of MMP-9 mRNA (300.4±66.1% of the control group, n=8, Fig. 14C) by quantitative real-time RT-PCR analysis. TIP inhibited UV-induced MMP-9 mRNA expressions (99.7±44.2% of the control group, n=8, Fig. 14C)

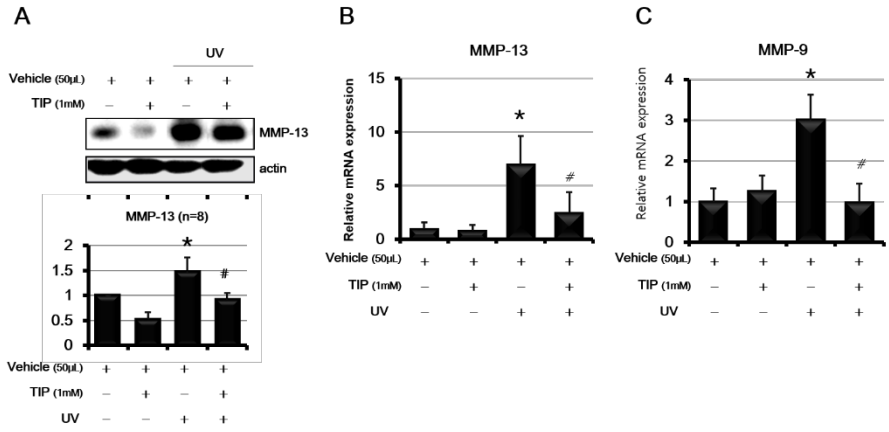

Figure 14. Down-regulation of UV-induced MMP-13 expression in hairless mice by treatment with TIP.

TIP (50 μL of 1 mM) was applied to the dorsal skin of mice at 0 (immediately after UV) and 24 hours after UV (200 mJ/cm^2, 1 time) irradiation. The skin of these mice were obtained at 48 hours after UV-irradiation. MMP-13 protein level was assessed by Western blotting. The bands shown are representative of their respective groups. Each level of MMP-13 protein was normalized to that of the corresponding β-actin, and their mean values ± SE are shown as bar graphs (Fig. 14A). MMP-13 and MMP-9 mRNA expressions were assessed by quantitative real-time RT-PCR analysis. The mRNA expression level of MMP-13 and MMP-9 was normalized versus that of the corresponding 36B4. Results are expressed as mean values ± SE. (Fig. 14B, 14C) *P<0.05 versus non-exposed vehicle-treated control mice, #P<0.05 versus UV-exposed vehicle-treated mice (n = 8)

TIP prevents UV-induced apoptosis.

To investigate whether TIP can prevent UV-induced apoptosis, I examined terminal dUTP nick-end labeling (TUNEL) assay for detecting cellular apoptosis after UV-irradiation.

I found that UV-irradiation caused apoptosis significantly in hairless mice and this UV-induced apoptosis was decreased by TIP (Fig. 15)

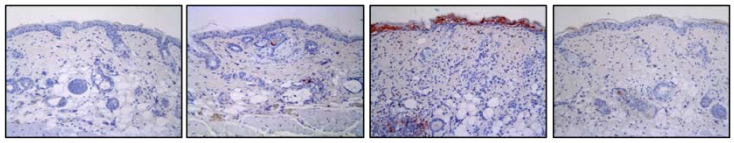

Vehicle (50μl)	+	+	+	+
TIP (1mM)	–	+	–	+
UV	–	–	+	+

Figure 15. TIP decreases UV-induced apoptosis.

TIP (50 μL of 1 mM) was applied to the dorsal skin of mice at 0 (immediately after UV) and 24 hours after UV (200 mJ/cm^2, 1 time) irradiation. These mice were biopsied at 48 hours after UV-irradiation. The effect of TIP on UV-induced cellular apoptosis was examined by terminal dUTP nick-end labeling (TUNEL staining, red spots) assay in hairless mice (n=8).

TIP inhibits UV-induced MMP-1 expression in human skin.

This clinical trial was designed to investigate the effect of TIP in photo-damaged human skin. Two MED of UV was irradiated on human buttock skin. To increase the penetration effect of TIP [54, 55], palmitoyl acid was linked to TIP, and I compared the effect of TIP with that of palmitoyl acid-linked TIP in human skin. To investigate the effect of TIP on UV-induced MMP-1 expression in human skin, I examined the protein level of MMP-1 expression. I found that UV exposure significantly increased the expressions of MMP-1 protein by Western blotting (613.43±54.79%, n=8; Fig. 16A).

TIP and also palmitoyl acid-linked TIP (PA-TIP) inhibited UV-induced MMP-1 expressions (33.32±15.84%, 29.27±27.30%, respectively, n=8; Fig. 16A).

Quantitative real-time RT-PCR analysis also showed that UV increased the mRNA level of IL-1β (369.8±94.0% of the control group, n=8, Fig. 16B) and PA-TIP decreased that of UV-induced IL-1β (235.0±48.0% of the control group, n=8, Fig. 16B).

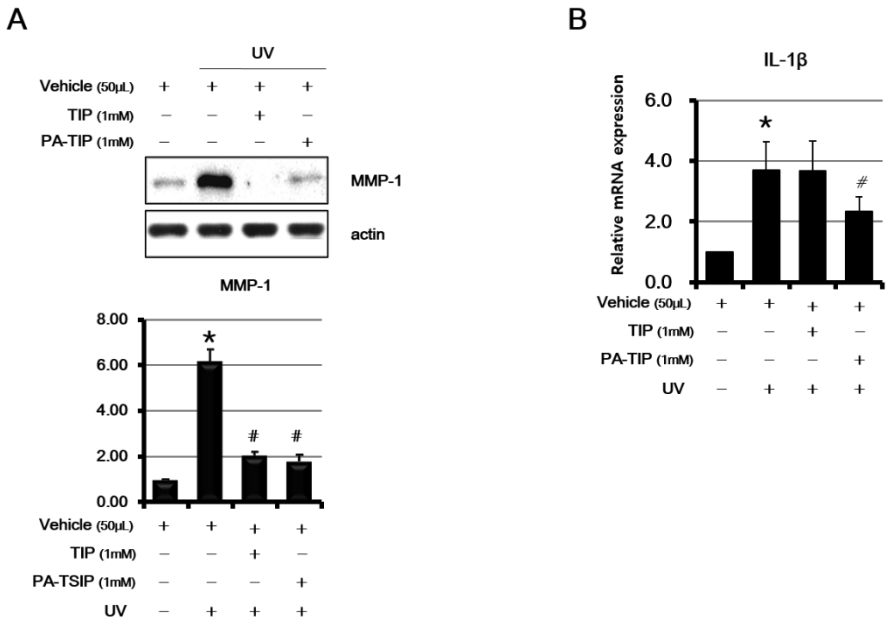

Figure 16. TIP decreases UV-induced MMP-1 expression in human skin.

TIP (25 μL of 1 mM, 1 time) was applied to the buttock skin of human immediately after single UV (140-180 mJ/cm^2) irradiation. Buttock skin of each subject was obtained at 24 hours after UV-irradiation.

The effect of TIP and also palmitoyl acid TIP (PA-TIP) on UV-induced MMP-1 protein level was assessed by Western blotting. The bands shown are representative of their respective groups. Each level of MMP-1 protein was normalized to that of the corresponding β-actin, and their mean values ± SE are shown as bar graphs (Fig. 16A, lower panels). *P<0.05 versus non-exposed vehicle-treated control skin, $^{\#}$P<0.05 versus

UV-exposed vehicle-treated skin (n = 8). IL-1β mRNA expression was assessed by quantitative real-time RT-PCR analysis. The mRNA expression level of IL-1β was normalized versus that of the corresponding 36B4. Results are expressed as mean values ± SE. (Fig. 16B) *P<0.05 versus non-exposed vehicle-treated control mice, $^{\#}$P<0.05 versus UV-exposed vehicle-treated mice (n = 8)

DISCUSSION

TRPV1 channel is a non-specific cation channel belonging to TRP family, which is activated by capsaicin and plays a role as a membrane protein to form membrane potential by calcium influx to send a stimulus to nerve system. The activation of TRPV1 is regulated by different pathways, which is exemplified by phosphorylation/dephosphorylation, including PKA, PKC, Ca^{2+}/calmodulin-dependent protein kinase (CaMKII), and Src kinase [74]. In addition, it was also suggested that TRPV1 regulates the heat- and ultraviolet (UV)-induced matrix metalloproteinases-1 (MMP-1) expression in human keratinocytes *in vitro*. Also, the expression level of TRPV1 proteins was increased by heat and UV stimulus in human skin *in vivo*. TRPV1 expression was increased in the photoaged (forearm) skin of the elderly compared to their sun-protected skin. However, little is known about the initial mechanism of UV-induced TRPV1's activation. Based on these functional roles about basal mechanism of TRPV1 after photo-stimulus, TRPV1 could be a novel target for anti-skin aging. In this study, I found that the TIP can act as a novel blocker for anti-skin aging, which mimics the activation sites in TRPV1 and competes with endogeneous TRPV1 (data not shown). These peptides correspond to the peptide sequences including 5 to 9 amino acids including Thr^{705} residue of TRPV1 phosphorylated by PKC and CaMKII (Fig. 7). Among them, the TRPV1 inhibitory peptide (TIP) could prevent

TRPV1 activation very effectively.

Since the C-terminal activation site (Thr^{705}) of TRPV1 sequences is localized in cytosol, TIP is able to play a blocking role when it is localized in cell cytosol. To confirm whether this peptide composed of 9 amino acid sequences could enter through cell membrane, FITC-linked peptide (FITC-TIP) was made. And I observed that TIP was able to go through cell membrane, which was independent of UV-irradiation (Fig. 12). This result suggests that the length of TIP (9 amino acids) are not too long to go through cell membrane [85, 86].

Our previous study showed that various TRPV1 blockers, such as capsazepine, 5'-iodoresiniferatoxin (I-RTX), and ruthenium red, can inhibit heat or UV responses in HaCaT cells [122]. Especially, the well-known TRPV1 blocker, 5' iodoresiniferotoxin (I-RTX), can inhibit UV-induced responses in a mouse model. Nevertheless, these blockers may not be safe enough to use in human skin, since these known inhibitors may be toxic or not be only specific to TRPV1 signaling. The sequence of TIP used in this study is 100% specific to TRPV1 [Blast: 4WX2UKT001R], so it cannot be excluded that TIP may affect on the PKC or CAMK signaling pathway. Moreover, peptides are considered to be very safe for human use [86, 123, 124].

If TRPV1 channel is activated, many amino acids such as tyrosine, serine,

and threonine were phosphorylated [74]. Since TIP targets phospho-threonine^{705} of TRPV1, it is necessary to confirm that TIP could inhibit the TRPV1 phosphorylation; Therefore as a further study, it should be investigated that the phosphorylation of threonine^{705} of TRPV1 is blocked by TIP. In this study, I examined the inhibitory effect of TIP indirectly.

I confirmed the effect of TIP to block the activation of TRPV1 by measuring calcium influx. In a previous study, our group has shown that calcium influx through TRPV1 plays a significant role in UV-induced downstream signaling, leading to MMP and pro-inflammatory cytokine expressions [37]. Since excessive amount of TIPs may inhibit phosphorylation of TRPV1, it may block the activation of endogeneous TRPV1, which makes TRPV1 channel open and calcium influxed. Therefore the inhibition of calcium influx by TIP could block efficiently the downstream signaling resulting in expressions of MMPs or pro-inflammatory cytokines.

Based on this effective inhibition of TIP in UV-induced responses from cell to mouse skin, TIP could be a potent blocker in UV-induced skin damage and may provide an effective therapeutic method for counteracting photoaging.

Chapter III.

Microarray analysis reveals the increased expression of nervous system-related genes in the aged human skin.

ABSTRACT

There are several nerve fibers in the skin. These nerve fibers may be regulated and changed by aging process. Several factors including neuronal growth factor (NGF) or brain-derived neurotrophic factor (BDNF) regulate neuronal outgrowth, and these nerve fibers play very important roles related with sensor, motor, pain, and various diseases. The nerve fibers are affected and changed by intrinsic aging. However, aging-related changes of nerve fibers in the skin are not fully understood. To detect and characterize the nervous system-related genes, transcriptome analysis using young and aged human skin was performed, and 23 nervous system-related differentially expressed genes were identified in the aged skin. Among those 23 genes, 6 nervous system related-genes were validated, (neurexophilin 3, small EDRK-rich factor 1A (telomeric) (small EDRK), neuropeptide Y receptor Y2 (NPY2R2), angiotensin II receptor, type 2 (ANG2R2), regulating synaptic membrane exocytosis 3 (RIMS3), and complexin 1) were increased in the aged skin. Additionally other well-known neuronal outgrowth factors (BDNF and NGF) and neurofilaments including neurofilament heavy chain (NF200), neurofilament light chain (NF68), and well-known neurofilament marker protein (PGP9.5.) were also increased in the aged skin.

I focused on tachychinin precursor 1 (TAC1) gene, from which substance P is expressed by alternative spicing. Substance P induces itch as a down signaling factor of TRPV1 in skin. The mRNA expression of substance P was significantly increased in the aged skin, and the receptor of substance P, neurokinin 1 receptor (NK1R) was also increased in fibroblasts from the aged skin. These results suggest that substance P may be a crucial factor in the development of senile pruritus.

Taken together, these data may provide a novel insight into the changes of nervous system related genes by aging.

Keywords: intrinsic skin aging, neuronal outgrowth factors, substance P, senile pruritus

MATERIALS AND METHODS

Materials

Capsaicin (M2028), anti-neurofilament light chain antibody (NF68, N5139), and anti-neurofilament heavy chain antibody (NF200, N4142) were purchased from Sigma Aldrich (St. Louis, MO). Rabbit polyclonal antibody against cannabinoid receptor 1 (CB1R, ab23703) and rabbit polyclonal antibody against cannabinoid receptor 2 (CB2R, ab3561) were supplied by abcam (Cambridge, UK). Goat polyclonal antibody against TRPV1 (sc-12498) and Goat polyclonal antibody against actin (sc-1616) were supplied by Santa Cruz Biotechnology (Santa Cruz, CA). Rabbit polyclonal antibody against PGP 9.5 (neurofilament marker, ADI-905-520-1) was purchased from ENZO Life Science (Farmingdale, NY, USA). Mounting solution with DAPI (VECTASHIELD Mounting Media for Fluorescence, H1200) was acquired from VECTOR Laboratories (Burlingame, CA). Donkey anti-goat IgG Alexa Fluor® 488 (A11055), and goat anti-rabbit IgG Alexa Fluor® 594 (A-11012) were acquired from Life technologies (Rockville, MD). The cell culture media and antibiotics were purchased from Life Technologies (Rockville, MD). Fetal bovine serum (FBS) was obtained from Hyclone (Logan, UT).

Methods

1. Cell culture and treatments

Human dermal fibroblasts, isolated from young and aged buttock skins, and the immortalized human keratinocytes cell line, HaCaT, were cultured in DMEM supplemented with glutamine (2 mM), penicillin (400 U/ml), streptomycin (50 mg/ml), and 10% FBS in a humidified 5% CO_2 atmosphere at 37 °C. Cultured human dermal fibroblasts were used at passages 6–10 for the experiments. For treatment of capsaicin desolved in DMSO, HaCaT cells were cultured to 80% confluence and then starved in DMEM containing 0% FBS for 24 hours. After treatment, cells were further incubated in the culture media containing at the indicated concentrations.

2. Human skin samples

Young Koreans (age range 20–35 years, n=13) and elderly Koreans (age range 71–90 years, n=13) without current or prior skin disease provided either upper-inner arm or buttock skin. Either 6-mm punch biopsy specimens were obtained from sun-protected upper-inner arm or buttock skin. This study was approved by the Institutional Review Board at the Seoul National University Hospital, and all subjects provided written informed consent.

3. Microarray analysis

The young and aged buttock skin samples were obtained from four patients by shave biopsy and isolated with dermal skin. The isolated and purified cRNA from each tissue was labelled according to the manufacturer's recommendations and hybridized on to Affymetrix Human U133 Plus 2.0 arrays (Affymetrix, Santa Clara, CA, U.S.A.), which cover 47400 transcripts and 38500 genes across the entire human genome. CEL files produced by GeneChip Operating System (Affymetrix) were imported to Affymetrix Expression Console Software (version 1.1.2) using a Microarray Suite 5 (MAS5) normalization preprocessor.

I filtered out probe sets with normalized values in all samples exhibiting < 20% intensity. Then, along with filtering by detection calls, pairwise comparisons between the young and aged skin were carried out to identify nervous system related genes (usually up-regulated, with twofold or greater changes in expression). The dataset is accessible in Gene Expression Omnibus (GEO series accession number GSE22998).

4. Western blot analysis

In order to measure protein level of CB1R, CB2R, NF 68, NF 200, PGP 9.5 in human skin, after skin samples were obtained from each subject by punch biopsy, the samples were incubated at 58°C for 2 minutes in phosphate-buffered saline (PBS), and epidermis and dermis were

separated with forceps. Skin samples were homogenized and extracted with lysis buffer containing 50 mm Tris–HCl (pH 7.4), 1% Triton X-100, 150 mm NaCl, 1 mm EDTA, 1 mm EGTA, 10 μg/ml aprotinin, 10 μg/ml leupeptin, 5 mm phenylmethylsulphonyl fluoride and 1 mm dithiothreitol. The protein content was determined using Bradford reagent (Bio-Rad, Hercules, CA, USA). Equal amounts (40 μg) of the protein samples were fractionated, transferred and analysed by Western blotting using each antibody. As a control, the corresponding β-actin levels were determined in the same cell lysates using the antibody for β-actin (Santa Cruz Biotechnology, SantaCruz, CA, USA).

5. Quantitative real-time RT-PCR

In order to measure mRNA of neurexophilin 3, small EDRK-rich factor 1A (telomeric) (small EDRK), neuropeptide Y receptor Y2 (NPY2R2), angiotensin II receptor, type 2 (ANG2R2), regulating synaptic membrane exocytosis 3 (RIMS3), complexin 1, and tachykinin, precursor 1 (substance P, SP), brain-derived neurotrophic factor (BDNF), nerve growth factor (NGF), cannabinoid receptor 1 and 2 (CB1R, CB2R), short and long form of neurokinin 1 receptor (NK1R), and TRPV1 in human, skin samples were obtained from each subject by punch biopsy, the samples were incubated at 58°C for 2 minutes in PBS and epidermis and dermis were separated with forceps. Total RNA was prepared from skin tissue using Trizol reagent according to the manufacturer's protocol

(Life Technologies, Rockville, MD, USA). The isolated RNA samples were electrophoresed in 1% agarose gels to assess the quality and quantity. One microgram of total RNA was used in a 20-μL first-strand cDNA synthesis reaction using a first-strand cDNA synthesis kit for RT-PCR according to the manufacturer's instructions (MBI Fermentas, Vilnius, Lithuania). For quantitative estimation of mRNA expression, PCR was performed on a 7500 Real-time PCR System (Applied Biosystems, Foster City, CA) using the SYBR Premix Ex TaqTM (Takara Bio Inc., Shiga, Japan), according to the manufacturer's instructions. Primers used were indicated in Table 2. PCR conditions were 50°C for 2 minutes, 95°C for 2 minutes, followed by 40 cycles at 95°C for 15 seconds and 60°C for 1 minutes. Data were analyzed using the 2-ΔΔCT method [29]; data were presented as the fold in gene expression normalized to 36B4.

6. Immunofluorescence

For immunofluorescence staining, human dermal fibroblasts were seeded in 4-well chamber slides (Falcon, BD Biosciences, Bedford, MA) with 1.5 x 10^4 cells per well and incubated for 48 hours. Cells were fixed in 4% paraformaldehyde in phosphate-buffered saline (PBS) for 30 minutes. Fixed cells were blocked with blocking solution (10% goat serum, 0.5% gelatin and 0.1% Triton X-100 in PBS) for 30 minutes and then

incubated with rabbit polyclonal antibody against CB1R diluted with blocking solution for overnight. The primary antibody treated cells were washed 3 times with PBS and incubated with fluorescein-conjugated secondary antibodies (Alexa Fluor®) diluted in blocking solution for 1 hour. Subsequently, the coverslips were mounted onto slides. Cells were observed under the fluorescence microscope (Carl Zeiss, Jena, Germany). Specimens were visualized with 405, 488, 545 nm lasers

For immunofluorescent staining of human skin, the biopsy samples were fixed in 10% buffered formaldehyde for 24 hours and embedded in paraffin wax. Sections (4 µm) were cut from the buttock skin specimens. After being deparaffinized in xylene, samples were dehydrated through a descending gradient of ethanol. After several washes in PBS, the endogenous peroxidase activity was quenched using 3% hydrogen peroxide for 6 minutes. The sections were then blocked with blocking solution (Zymed) for 30 minutes, then washed and incubated with the primary goat polyclonal antibody against TRPV1 in a humidified chamber at 4°C for 18 hours. After washing in PBS, the sections were incubated with secondary donkey anti-goat IgG Alexa Fluor® 488 for 1 hour at room temperature. The nuclei were counterstained by DAPI staining. All the sections were examined immediately and photographed with a Zeiss LSM 510 META confocal laser scanning microscope (Zeiss, Yena, Germany)

Table 2. Primer sequences for human genes for quantitative real-time PCR.

Human gene	5' primer sequence	3' primer sequence
36B4	TCG ACA ATG GCA GCA TCT AC	TGA TGC AAC AGT TGG GTA GC
neurexophillin 3	TGC AGC GCA GAG TTG GGT GG	TGA ACG GCA CAC GGT GGG TG
RIMS 3	TGG GAC CAC CAC CGC CAA GA	GTG CCG TCG GAG CTG TTG CT
small EDRK	TCC AGG CTC CGT TGG GGG TC	TTC ATG TTT TTC TGG CGG GCA AGT
NPY2R2	CGC TGT GAG CAG CGG TTG GA	GCC AAG CAG GGA GCA GCG AA
complexin 1	TGG GCT CCA AGC AGA TGC	GGC TTC GCT GGC TCC CAC
ANG2R2	GGC AAC TCC ACC CTT GCC ACT	ACA CCC ATC CAG GCC AGA GCA T
spectrin	AGA GCG AGC AAA AGG CGC GA	AGA ACT TCT CCA GGC ATC TTC TGG T
Contactin	ATG CTC CGA CAG GTG GCC CT	TGA CGC AGC CCG AGG CAA TG
BDNF	AAC AAT AAG GAC GCA GAC TT	TGC AGT CTT TTT GTC TGC TGC CG
NGF	CAG GAC TCA AAG GAG CAA GC	CAG GAC TCA AAG GAG CAA GC
CB1R	AAG ACC CTG GTC CTG ATC CT	TGG CAA TCT TGA CTG TGC TC
CB2R	ATG GGC ATG TTC TCT GGA AG	GGG CTT CTT CTT TTG CCT CT
UCHL 1	TGC TGA ACA AAG TGC TGT CC	CAC AGG AAT TCC CAA TGG TC
NK1R short	TCT TCT TCC TCC TGC CCT ACA TC	GGT TGG GAT CCT CAC CTG TCA T
NK1R long	TCT TCT TCC TCC TGC CCT ACA TC	GCC CAG ACG GAA CCT GTC AT
TRPV1	TGT GCC GTT TCA TGT TT	TGC ACC TTC CAG ATG TT
SP	GCG GGA CTG TCC GTC GCA AA	AGC TCT TTT GCC CAT TAG TCC AAC AA

RESULTS

Nervous system-related genes are increased in the old human skin.

To identify the significant factors and to find various unexpected targets involved in intrinsic skin aging, a microarray analysis was performed using buttock dermal skin tissues obtained from the young and the aged. (9 subjects in each group, aged of 20-33 years and 71-90 years, respectively) Using the filtering criteria described on Materials and methods, 23 nervous system-related genes in the aged dermal skin were up-regulated as compared to the young dermal skin. They are neuropeptide Y receptor Y2, neuromedin U receptor 2, mab-21-like 2 (C. elegans), angiotensin II receptor, type 2, regulating synaptic membrane exocytosis 3, cerebellin 1 precursor, translocase of inner mitochondrial membrane 8 homolog A (yeast), complexin 1, Cysteine rich transmembrane BMP regulator 1 (chordin-like), Sortilin-related VPS10 domain containing receptor 1, Down syndrome cell adhesion molecule, leucine-rich repeats and calponin homology (CH) domain containing 4, Synaptosomal-associated protein, 25 kDa, Solute carrier family 6, member 16, Baculoviral IAP repeat-containing 1, contactin 2 (axonal), neurexophilin 3, synapsin II, Small EDRK-rich factor 1A (telomeric), amyloid beta (A4) precursor protein-binding, family A, member 2 (X11-

like), Spectrin repeat containing, nuclear envelope 2, tachykinin, precursor 1 (alternatively transcribed with substance K, substance P, neurokinin 1, neurokinin 2, neuromedin L, neurokinin alpha, neuropeptide K, neuropeptide gamma), and Atrophinatrophin 1. These genes were increased in the old dermal skin with two-fold or greater changes in expression, as compared with the young dermal skin. (Table. 3)

To validate the microarray data, quantitative real-time RT-PCR analysis of these upregulated 23 genes was performed, and the mRNA level of 6 targets was found to be increased in the old skin. The mRNA levels of neurexophilin 3, regulating synaptic membrane exocytosis 3 (RIMS3), small EDRK-rich factor 1A (telomeric) (small EDRK), neuropeptide Y receptor Y2 (NPY2R2), complexin 1, and angiotensin II receptor, type 2 (ANG2R2) were increased in the old skin (114.3±27.2%, 118.1±20.5%, 146.9±20.5%, 134.9±34.4%, 230.0±93.9%, 264.6±70.5% of the young skin, respectively; n=9, Fig. 17A). Two genes including spectrin and celebelin were increased in the old skin, albeit not significant (Fig. 17A). Quantitative real-time RT-PCR analysis of the genes in the old dermal skin was also performed, and the mRNA levels of 7 targets were increased similarly in the old dermal skin. The mRNA levels of neurexophilin 3, small EDRK-rich factor 1A (telomeric) (small EDRK), neuropeptide Y receptor Y2 (NPY2R2), angiotensin II receptor, type 2 (ANG2R2), regulating synaptic membrane exocytosis 3 (RIMS3), and complexin 1

were increased in the old skin (165.1±70.6%, 173.5±10.7%, 280.0±121.1%, 299.2±120.7%, 360.0±178.1%, 784.5±426.3% of the young skin, respectively; n=4, Fig. 17B). Two genes including celebelin and spectrin were increased in the old skin, albeit not significant (Fig. 17B). Additionally, the mRNA level of tachykinin, precursor 1 (substance P, SP) was also increased in the old dermal skin (423.0±154.5% of the young skin, n=4, Fig. 30B).

Table 3. Nervous system-related genes are increased in the old human skin.

	Increased nervous system related gene in human old dermis.	Average fold
1	neuropeptide Y receptor Y2	7.93
2	neuromedin U receptor 2	5.97
3	mab-21-like 2 (C. elegans)	5.07
4	angiotensin II receptor, type 2	4.83
5	regulating synaptic membrane exocytosis 3	4.12
6	cerebellin 1 precursor	3.71
7	translocase of inner mitochondrial membrane 8 homolog A (yeast)	3.67
8	complexin 1	3.58
9	Cysteine rich transmembrane BMP regulator 1 (chordin-like)	3.35
10	Sortilin-related VPS10 domain containing receptor 1	3.27
11	Down syndrome cell adhesion molecule	3.14
12	leucine-rich repeats and calponin homology (CH) domain containin g 4	2.89
13	Synaptosomal-associated protein, 25kDa	2.88
14	Solute carrier family 6, member 16	2.56
15	Baculoviral IAP repeat-containing 1	2.47
16	contactin 2 (axonal)	2.34
17	neurexophilin 3	2.31
18	synapsin II	2.24
19	Small EDRK-rich factor 1A (telomeric)	2.21
20	amyloid beta (A4) precursor protein-binding, family A, member 2 (X11-like)	2.21
21	Spectrin repeat containing, nuclear envelope 2	2.15
22	tachykinin, precursor 1 (substance K, substance P, neurokinin 1, ne urokinin 2,neuromedin L, neurokinin alpha, neuropeptide K, neuro peptide gamma)	2.01
23	Atrophin 1	2.00

The young and aged buttock skin samples were biopsied and dermal skin regions were isolated (n=4). The isolated and purified cRNA from each tissue was labelled according to the manufacturer's recommendations and hybridized on to Affymetrix Human U133 Plus 2.0 arrays (Affymetrix, Santa Clara, CA, U.S.A.). I filtered out probe sets with normalized values in all samples exhibiting < 20% intensity, and then, along with filtering by detection calls, pairwise comparisons between the young dermal skin and the old dermal skin were carried out to identify nervous system-related genes with two-fold or greater changes in expression.

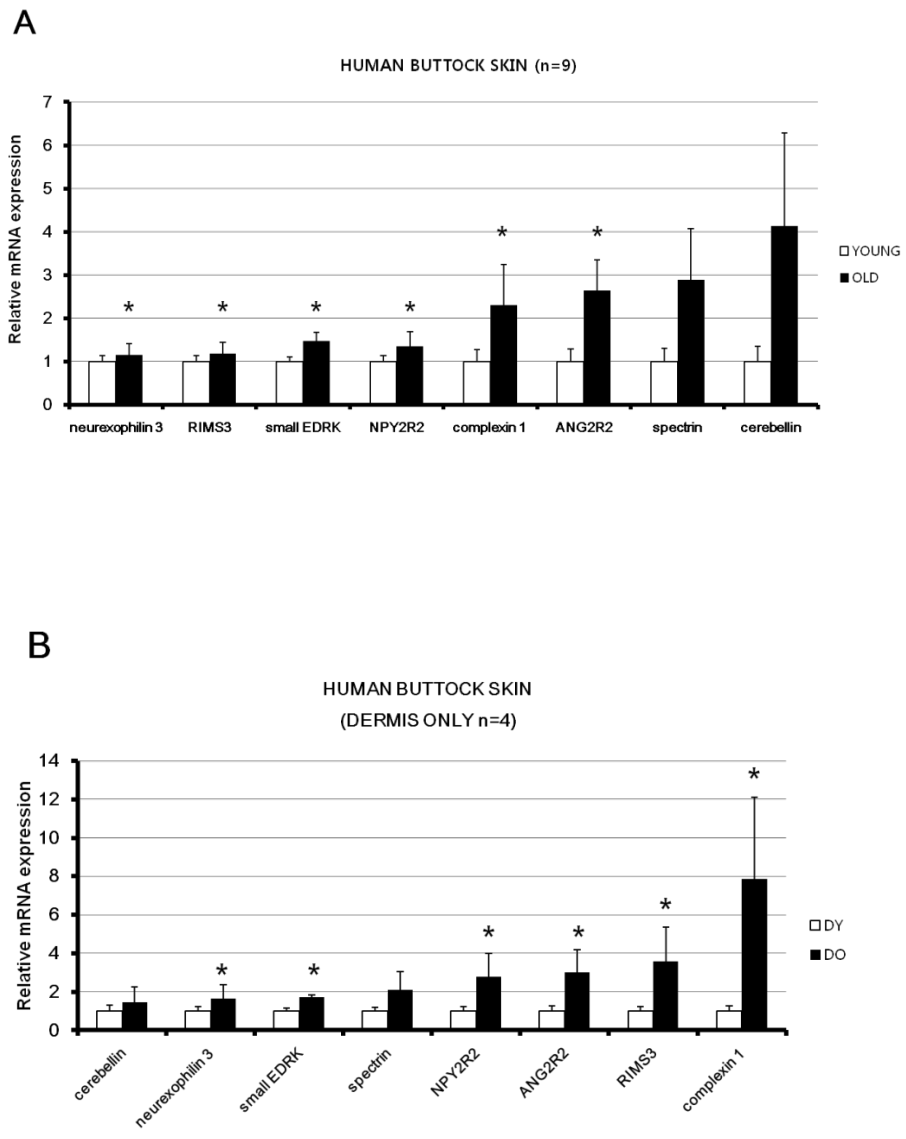

Figure 17. The increased expression of nervous-system related genes in the young and aged human skin *in vivo*.

For validation of microarray analysis, 23 selected genes differentially expressed in young and old skin, the mRNA levels were measured by real-time reverse transcription–polymerase chain reaction (RT-PCR) (Fig. 17A). Each level of mRNA was normalized versus that of the corresponding 36B4 mRNA. Results are expressed as mean values ± SE. *P < 0.05 versus the young group.

Total RNAs were isolated from young and old dermal skin were subjected to microarray analysis. The mRNA levels were measured by real-time RT-PCR (DY: dermal skin of the young, DO: dermal skin of the aged, Fig. 17B). Each level of mRNA was normalized versus that of the corresponding 36B4 mRNA. Results are expressed as mean values ± SE. *P < 0.05 versus the young group.

The neuronal outgrowth factors are increased in the old human skin.

To confirm that the aging process is related to neuronal outgrowth in skin, I investigated the changes in the mRNA and protein expressions of several neuronal outgrowth factors caused by intrinsic aging. I compared the expression of several targets well-known as neuronal outgrowth factors in the young and aged buttock skin. In the naturally-aged buttock skin of the elderly, the mRNA expression of brain-derived neurotrophic factor (BDNF) and nerve growth factor (NGF) were higher than in the buttock skin of young people (130.4 ± 38.6%, 226.4 ± 39.3% of the young skin, respectively, n = 9, Fig. 18A). To be more specific, I isolated the dermal skin region in the young and aged buttock skin, and found more prominent increase in neuronal outgrowth factors in the old dermal skin. The mRNA levels of brain-derived neurotrophic factor (BDNF), nerve growth factor (NGF), and cannabinoid receptor 1 and 2 (CB1R, CB2R) were increased in the old dermal skin (165.1 ± 35.3%, 202.4 ± 43.8%, 166.1 ± 52.9%, 196.4 ± 96.8% of the young skin, respectively, n = 4) (Fig. 18B). The mRNA levels of CB1R and CB2R were also increased in the primary cultured fibroblasts from the young and old buttock skin (133.2 ± 9.6%, 339.0 ± 70.6% of the young skin, respectively, n = 6, Fig. 18C).

The aged buttock skin of the elderly showed an increase in CB1R and CB2R protein expression compared to the young buttock skin as shown by Western blotting (n=4, Fig. 18D), and the protein expression of CB1R was also increased in the aged buttock dermal skin (n=4, Fig. 18E). Additionally, the immunofluorescence staining in the primary cultured fibroblasts from the young and aged buttock skin showed an increased expression of CB1R protein (n=3, Fig. 18F).

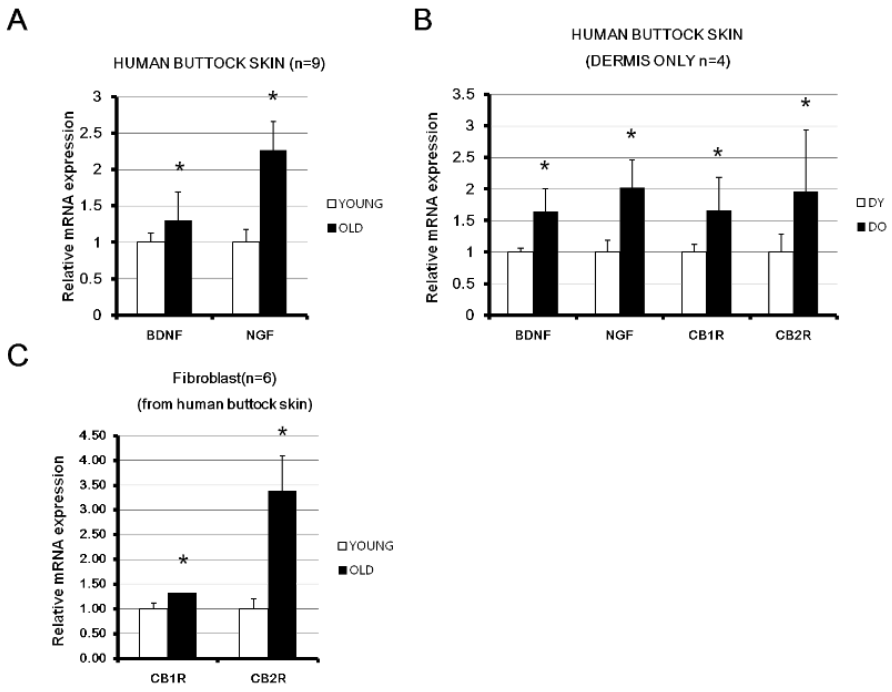
A
HUMAN BUTTOCK SKIN (n=9)
Relative mRNA expression
3
2.5
2
1.5
1
0.5
0
BDNF
NGF
YOUNG
OLD
B
HUMAN BUTTOCK SKIN
(DERMIS ONLY n=4)
Relative mRNA expression
3.5
3
2.5
2
1.5
1
0.5
0
BDNF
NGF
CB1R
CB2R
DY
DO
C
Fibroblast(n=6)
(from human buttock skin)
Relative mRNA expression
4.50
4.00
3.50
3.00
2.50
2.00
1.50
1.00
0.50
0.00
CB1R
CB2R
YOUNG
OLD

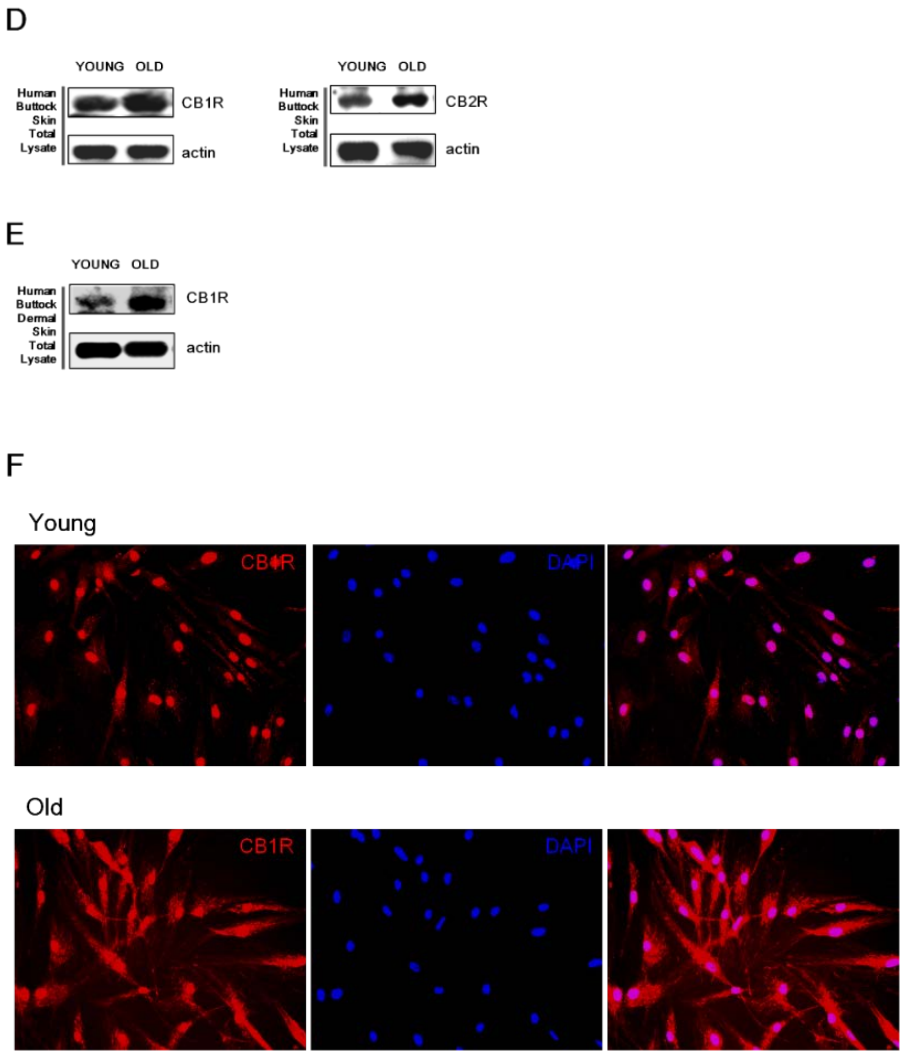

Figure 18. The neuronal outgrowth factors are incresed in the young and aged human skin *in vivo*.

The buttock skin of young (20 to 35-years old) and elderly subjects (72 to 89-years old) was obtained as described in Materials and methods. The mRNA levels of BDNF and NGF of the young and aged buttock skin were measured by real-time reverse transcription–polymerase chain reaction

(RT-PCR). Each level of mRNA was normalized versus that of the corresponding 36B4 mRNA. Results are expressed as mean values ± SE. $^{*}P < 0.05$ versus the young group. (n = 9, Fig. 18A). The mRNA levels of BDNF, NGF, CB1R, and CB2R of the isolated young and aged buttock dermal skin were measured by real-time RT-PCR. Each level of mRNA was normalized versus that of the corresponding 36B4 mRNA. Results are expressed as mean values ± SE. $^{*}P < 0.05$ versus the young group. (n = 4, DY: dermal skin of the young, DO: dermal skin of the aged, Fig. 18B). Primary fibroblasts were isolated from buttock skin of young (20 to 35-years old) and elderly subjects (72 to 89-years old). The mRNA levels CB1R and CB2R of fibroblasts from the young and aged buttock skin were quantitated by real-time RT-PCR. Each level of mRNA was normalized versus that of the corresponding 36B4 mRNA. Results are expressed as mean values ± SE. $^{*}P < 0.05$ versus the young group. (n = 9, Fig. 18C). CB1R and CB2R protein of the young and aged buttock skin were observed by Western blotting. The bands shown are representative of their respective groups. (Fig. 18D). The CB1R protein of the isolated young and aged buttock dermal skin was determined by Western blotting. The bands shown are representative of their respective groups. (Fig. 18E).

CB1R expression was increased in the fibroblasts isolated from the old skin. The primary fibroblasts were cultured from buttock skin of young (20 to 35-years old, the upper figures, Fig. 18F) and elderly subjects (72

to 89-years old, the lower figures, Fig. 18F). The fibroblasts were fixed and stained using aan anti-CB1R antibody (red, Fig. 18F). Nuclei were counterstained with 4',6-diamidino-2-phenylindole (DAPI, blue). HaCaT cells were photographed with a Zeiss LSM 510 META confocal laser-scanning microscope (Zeiss, Yena, Germany) (n=5, Fig. 18F).

The expressions of neurofilaments are increased in the old human skin.

Based on these data, to confirm that neurofilament expression is affected by aging process in skin, I investigated the changes in the expression level of neurofilaments in the young and aged skin. In the naturally-aged buttock skin of the elderly, the mRNA expression of ubiquitin carboxy-terminal hydrolase L1 (UCHL1), known as a neurofilament marker, was higher than in the buttock skin of young people (167.7 ± 44.6% of the young skin, n = 9, Fig. 19A). I also investigated the expression of neurofilaments using Western blotting with several neurofilament markers or antibodies. The Western blotting results showed an increase of nerufilamentneurofilament heavy chain antibody (NF200), neurofilament light chain (NF68), and a well-known neurofilament marker (PGP 9.5) protein expression in the elderly skin compared to the young buttock skin (n=4, Fig. 19B), and all of these protein expression was also increased in the aged buttock dermal skin (n=4, Fig. 19C).

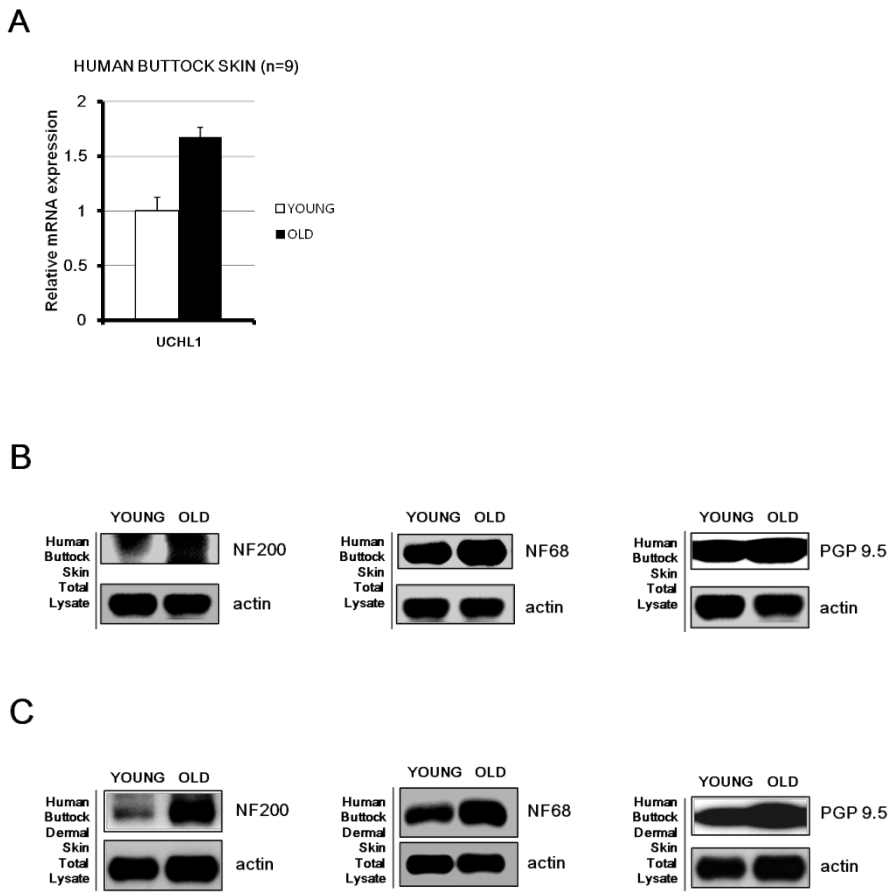

Figure 19. The neurofilaments are incresed in the young and aged human skin *in vivo*.

The buttock skin of young (20 to 35-years old) and elderly subjects (72 to 89-years old) was biopsied as described in Materials and methods. The mRNA levels UCHL1 of the young and aged buttock skin were measured by real-time RT-PCR. Each level of mRNA was normalized versus that of the corresponding 36B4 mRNA. Results are expressed as mean values ±

SE. *P < 0.05 versus the young group (n = 9, Fig. 19A). The protein levels of 200 kDa of neurofilament heavy chain (NF 200), 68 kDa of neurofilament light chain (NF 68), and neurofilament marker PGP 9.5 from the young and aged buttock skin were observed by Western blotting. (n = 4, Fig. 19B, 19C).

TRPV1 are increased in the aged human skin *in vivo*, and mRNA level of the itch-related factors including substance P and the receptor of substance P (NK1R) are increased.

TRPV1 signaling is involved in itch as followed by the release of substance P from c-fiber, which is recently studied as another cause of itch apart from histamine-induced signaling [50]. Moreover, according to the previous study, the expression of TRPV1 is increased in the aged skin compared to the young skin [37]. Thus I investigated whether TRPV1-induced itch signaling is related to the aging process.

I investigated the changes in the mRNA and protein expressions of TRPV1-induced itch signaling molecules caused by intrinsic aging. I compared the expression of neurokinin 1 receptor (NK1R), known as substance P receptor, in the young and aged buttock skin. In the naturally-aged buttock skin of the elderly, the mRNA expressions of NK1R and TRPV1 were higher than those in the buttock skin of the young (132.1 ± 17.9%, 137.9 ± 29.0% of the young skin, respectively, n = 9, Fig. 20A). To be more specific, the dermal skin was isolated in the young and aged buttock skin, and TRPV1-induced itch signaling molecules were found to be more increased in the old dermal skin. The mRNA levels of the short form and long form of NK1R, TRPV1, and

substance P were increased in the old dermal skin (237.6 ± 89.3%, 203.7 ± 36.0%, 225.1 ± 63.2%, 433.0 ± 154.5% of the young skin, respectively, n = 4, Fig. 20B). The mRNA levels of the short form and long form of NK1R were also increased in the primarily-cultured fibroblasts from the young and old buttock skin (213.4 ± 43.2%, 615.9 ± 0.9% of the young skin, respectively, n = 6, Fig. 20C).

The buttock skin of the elderly showed an increase in TRPV1 as reported in the previous study (Fig. 20D), and the protein expression of TRPV1 was also increased in both aged buttock dermal skin as well as the aged buttock skin (n=4, Fig. 20E, 20F).

Additionally, I investigated whether the receptor of substance P, NK1R is increased by TRPV1 activation. HaCaT cells were pretreated with TRPV1 agonist, capsaicin for 30 minutes, then the culture dishes were incubated for 48 hours. Quantitative real-time RT-PCR analysis showed an increase in NK1R mRNA in a dose-dependent manner. Both 20 and 30 μM of capsaicin induced the expression of NK1R (431.7±50.1%, 397.6±49.1% of the control group, n=3, Fig. 20G).

A

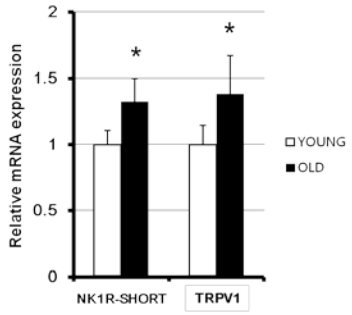
HUMAN BUTTOCK SKIN (n=9)
Relative mRNA expression
2
1.5
1
0.5
0
*
*
YOUNG
OLD
NK1R-SHORT
TRPV1

B

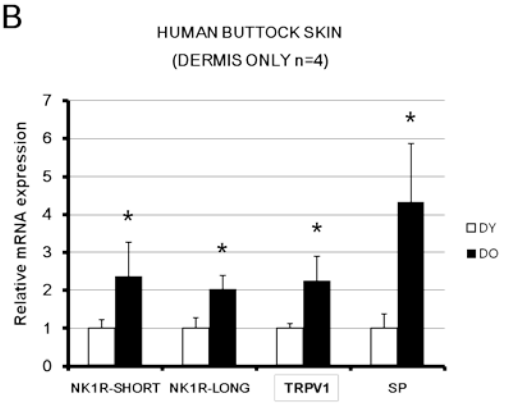
HUMAN BUTTOCK SKIN
(DERMIS ONLY n=4)
Relative mRNA expression
7
6
5
4
3
2
1
0
*
*
*
*
DY
DO
NK1R-SHORT
NK1R-LONG
TRPV1
SP

C

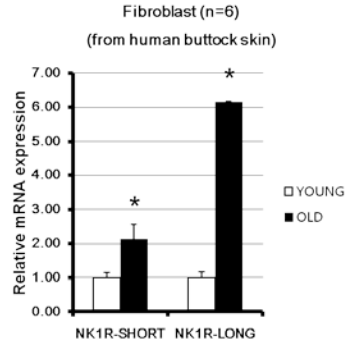
Fibroblast (n=6)
(from human buttock skin)
Relative mRNA expression
7.00
6.00
5.00
4.00
3.00
2.00
1.00
0.00
*
*
YOUNG
OLD
NK1R-SHORT
NK1R-LONG

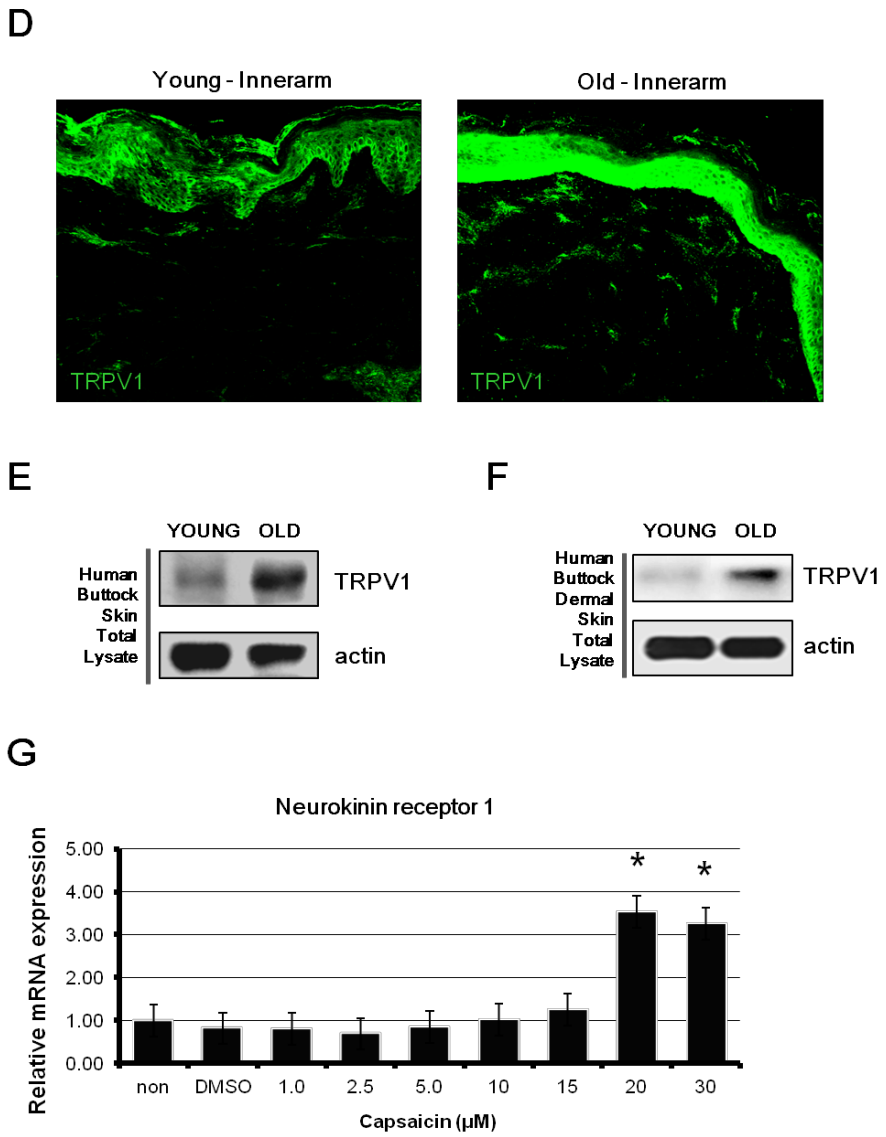

Figure 20. TRPV1 are increased in the aged human skin *in vivo*, and mRNA level of the itch-related factors including substance P and the receptor of substance P (NK1R) are increased.

The buttock skin of young (20 to 35-years old) and elderly subjects (72 to 89-years old) was biopsied as described in Materials and methods. The mRNA levels of short form of NK1R and TRPV1 of the young and aged buttock skin were measured by real-time RT-PCR. Each level of mRNA was normalized versus that of the corresponding 36B4 mRNA. Results are expressed as mean values ± SE. $^{*}P < 0.05$ versus the young group (n = 9, Fig. 20A). The mRNA levels of short form and long from of NK1R, TRPV1, and substance P of the separated young and aged buttock dermal skin were measured by real-time RT-PCR. Each level of mRNA was normalized versus that of the corresponding 36B4 mRNA. Results are expressed as mean values ± SE. $^{*}P < 0.05$ versus the young group (n = 9, DY: dermal skin of the young, DO: dermal skin of the aged, Fig. 20B). The fibroblasts were primary cultured from buttock skin of young (20 to 35-years old) and elderly subjects (72 to 89-years old) was biopsied as described in Materials and methods. The mRNA levels of short form and long from of NK1R in fibroblasts from the young and aged buttock skin were measured by real-time RT-PCR. Each level of mRNA was normalized versus that of the corresponding 36B4 mRNA. Results are expressed as mean values ± SE. $^{*}P < 0.05$ versus the young group (n = 9, Fig. 20C). The TRPV1 protein was immuno-stained using a rabbit-polyclonal antibody against TRPV1 in young and aged sun-protected upper-inner arm skin *in vivo* (Fig. 20D). The protein levels of TRPV1 from the isolated young and aged buttock skin or the young and aged

buttock dermal skin were observed by Western blotting (n = 4, Fig. 20E, 20F). HaCaT cells were cultured in 60 mm dish. Culture media was changed with serum-free media and incubated for 24 hours. After pretreatment with the TRPV1 agonist, capsaicin, for 30 minutes, the cultured HaCaT cells incubated for 48 hours with fresh media containing capsaicin. The mRNA level of NK1R was measured by real-time RT-PCR. The mRNA was normalized versus that of the corresponding 36B4 mRNA (n=3, Fig. 20G). Results are expressed as mean values ± SE. $^{*}P < 0.05$ versus the control group.

DISCUSSION

TRPV1 channel is expressed not only in neuronal cells in the brain, but also in keratinocytes in the epidermis, and there are a sophisticated network of nerve fibers in the skin. These nerve fibers may be regulated and changed by aging process. Several factors including nerve growth factor (NGF) or brain-derived neurotrophic factor (BDNF) regulate neuronal outgrowth, and these nerve fibers play very important roles related with sensor, motor, pain, and various neuronal diseases [44, 46, 49, 125, 126]. The nerve fibers are affected and changed by intrinsic aging. However, the aging-related changes of nerve fibers in the skin are not fully understood.

In this study, I provided that neuronal growth factors including NGF and BDNF were increased in the aged skin. And well-known other neurogenesis factors cannabinoid receptor 1 and 2 were also increased in the aged people. These results imply that adult neurogenesis is caused by aging process in skin as a complementary system for the attenuated sensing.

In this study, neurofilament light chain (NF 68) and neurofilament heavy chain (NF 200) were also increased in the aged skin. And I confirmed this neurofilament increase in the aged skin by showing that another neurofilament marker, PGP 9.5 was increased in the aged skin. As

further study, it is need to identify the mechanism or cause of adult neurogenesis in skin.

Our group identified 23 differentially-expressed, nervous system-related genes in the aged skin. Among those 23 genes, 6 nervous system related genes were validated. Other genes seemed to be increased also, therefore they thought to be increased significantly by increasing the number of samples. Since the 6 nervous system-related genes were not well studied yet, therefore finding out the function or role of the genes in human skin can be valuable things.

The aged skin exhibited an increased expression of other well-known neuronal outgrowth factors such as tachychinin precursor 1 (TAC1) gene, from which substance P is expressed by alternative spicing [38, 108, 127]. Itch, the sensation of desire to scratch is induced by SP. SP, as the most potent pruritogenic endogenous peptides, causes the degranulation and itch induced by SP is thought to be mediated by its upstream signaling molecule, TRPV1 through c-fiber, known as pain sensing neurofilament. In this study, the mRNA expression of substance P is increased in the aged skin significantly, and the receptor of substance P, neurokinin 1 receptor (NK1R) is also increased in the old fibroblasts. These results imply that senile pruritus may be caused by the increase of substance P and its receptor, NK1R in human skin. Although most of the elderly people suffer from the senile pruritus, the therapy for senile pruritus is

insufficient yet [38, 108, 127]. Therefore these data provides that targeting substance P could be a potent strategy for senile pruritus treatment. Moreover, since the increased expression level of TRPV1 may be a significant factor causing the increase of substance P, TRPV1 could be also a potent target in this elderly irritating symptom. In this study, our results provide that substance P may be a crucial factor in senile pruritus. To confirm this, it is need to compare the expression level of substance P, NK1R, or TRPV1 in the skin from normal aged people and aged people who are suffered from senile pruritus.

REFERENCES

1. **Gilchrest, B.A. (1982). Age-associated changes in the skin. Journal of the American Geriatrics Society *30*, 139-143.**

2. **Gilchrest, B.A. (1989). Skin aging and photoaging: an overview. Journal of the American Academy of Dermatology *21*, 610-613.**

3. **Jenkins, G. (2002). Molecular mechanisms of skin ageing. Mechanisms of ageing and development *123*, 801-810.**

4. **Ma, W., Wlaschek, M., Tantcheva-Poor, I., Schneider, L.A., Naderi, L., Razi-Wolf, Z., Schuller, J., and Scharffetter-Kochanek, K. (2001). Chronological ageing and photoageing of the fibroblasts and the dermal connective tissue. Clinical and experimental dermatology *26*, 592-599.**

5. **Oikarinen, A. (1990). The aging of skin: chronoaging versus photoaging. Photodermatology, photoimmunology & photomedicine *7*, 3-4.**

6. **Lavker, R.M. (1979). Structural alterations in exposed and unexposed aged skin. The Journal of investigative dermatology *73*, 59-66.**

7. **Lavker, R.M., and Kligman, A.M. (1988). Chronic heliodermatitis:**

a morphologic evaluation of chronic actinic dermal damage with emphasis on the role of mast cells. The Journal of investigative dermatology *90*, 325-330.

8. Lucke-Huhle, C., Mai, S., and Herrlich, P. (1989). UV-induced early-domain binding factor as the limiting component of simian virus 40 DNA amplification in rodent cells. Mol Cell Biol *9*, 4812-4818.

9. Rittie, L., and Fisher, G.J. (2002). UV-light-induced signal cascades and skin aging. Ageing research reviews *1*, 705-720.

10. Stein, B., Kramer, M., Rahmsdorf, H.J., Ponta, H., and Herrlich, P. (1989). UV-induced transcription from the human immunodeficiency virus type 1 (HIV-1) long terminal repeat and UV-induced secretion of an extracellular factor that induces HIV-1 transcription in nonirradiated cells. J Virol *63*, 4540-4544.

11. Stein, B., Rahmsdorf, H.J., Steffen, A., Litfin, M., and Herrlich, P. (1989). UV-induced DNA damage is an intermediate step in UV-induced expression of human immunodeficiency virus type 1, collagenase, c-fos, and metallothionein. Mol Cell Biol *9*, 5169-5181.

12. Schonthal, A., Buscher, M., Angel, P., Rahmsdorf, H.J., Ponta, H., Hattori, K., Chiu, R., Karin, M., and Herrlich, P. (1989). The Fos

and Jun/AP-1 proteins are involved in the downregulation of Fos transcription. Oncogene *4*, 629-636.

13. Chen, Y.Q., Mauviel, A., Ryynanen, J., Sollberg, S., and Uitto, J. (1994). Type VII collagen gene expression by human skin fibroblasts and keratinocytes in culture: influence of donor age and cytokine responses. J Invest Dermatol *102*, 205-209.

14. Mauviel, A., Halcin, C., Vasiloudes, P., Parks, W.C., Kurkinen, M., and Uitto, J. (1994). Uncoordinate regulation of collagenase, stromelysin, and tissue inhibitor of metalloproteinases genes by prostaglandin E2: selective enhancement of collagenase gene expression in human dermal fibroblasts in culture. J Cell Biochem *54*, 465-472.

15. Varga, J., Li, L., Mauviel, A., Jeffrey, J., and Jimenez, S.A. (1994). L-Tryptophan in supraphysiologic concentrations stimulates collagenase gene expression in human skin fibroblasts. Lab Invest *70*, 183-191.

16. Mauviel, A., Lapiere, J.C., Halcin, C., Evans, C.H., and Uitto, J. (1994). Differential cytokine regulation of type I and type VII collagen gene expression in cultured human dermal fibroblasts. J Biol Chem *269*, 25-28.

17. Pentland, A.P., Shapiro, S.D., and Welgus, H.G. (1995). Agonist-induced expression of tissue inhibitor of metalloproteinases and metalloproteinases by human macrophages is regulated by endogenous prostaglandin E2 synthesis. J Invest Dermatol *104*, 52-57.

18. Valtonen, V., Karppinen, L., and Kariniemi, A.L. (1989). A comparative study of ciprofloxacin and conventional therapy in the treatment of patients with chronic lower leg ulcers infected with Pseudomonas aeruginosa or other gram-negative rods. Scand J Infect Dis Suppl *60*, 79-83.

19. Bernstein, E.F., Chen, Y.Q., Tamai, K., Shepley, K.J., Resnik, K.S., Zhang, H., Tuan, R., Mauviel, A., and Uitto, J. (1994). Enhanced elastin and fibrillin gene expression in chronically photodamaged skin. J Invest Dermatol *103*, 182-186.

20. Herschman, H.R., Xie, W., and Reddy, S. (1995). Inflammation, reproduction, cancer and all that.... The regulation and role of the inducible prostaglandin synthase. Bioessays *17*, 1031-1037.

21. Alcorta, D.A., Xiong, Y., Phelps, D., Hannon, G., Beach, D., and Barrett, J.C. (1996). Involvement of the cyclin-dependent kinase inhibitor p16 (INK4a) in replicative senescence of normal human fibroblasts. Proc Natl Acad Sci U S A *93*, 13742-13747.

22. **Buchman, C., Skroch, P., Welch, J., Fogel, S., and Karin, M. (1989). The CUP2 gene product, regulator of yeast metallothionein expression, is a copper-activated DNA-binding protein. Mol Cell Biol *9*, 4091-4095.**

23. **Bevan, S., Hothi, S., Hughes, G., James, I.F., Rang, H.P., Shah, K., Walpole, C.S., and Yeats, J.C. (1992). Capsazepine: a competitive antagonist of the sensory neurone excitant capsaicin. British journal of pharmacology *107*, 544-552.**

24. **Oh, U., Hwang, S.W., and Kim, D. (1996). Capsaicin activates a nonselective cation channel in cultured neonatal rat dorsal root ganglion neurons. Journal of Neuroscience *16*, 1659-1667.**

25. **Wood, J.N., Winter, J., James, I.F., Rang, H.P., Yeats, J., and Bevan, S. (1988). Capsaicin-induced ion fluxes in dorsal root ganglion cells in culture. Journal of Neuroscience *8*, 3208-3220.**

26. **Seabrook, G.R., Sutton, K.G., Jarolimek, W., Hollingworth, G.J., Teague, S., Webb, J., Clark, N., Boyce, S., Kerby, J., Ali, Z., et al. (2002). Functional properties of the high-affinity TRPV1 (VR1) vanilloid receptor antagonist (4-hydroxy-5-iodo-3-methoxyphenylacetate ester) iodo-resiniferatoxin. The Journal of pharmacology and experimental therapeutics *303*, 1052-1060.**

27. Tominaga, M., Caterina, M.J., Malmberg, A.B., Rosen, T.A., Gilbert, H., Skinner, K., Raumann, B.E., Basbaum, A.I., and Julius, D. (1998). The cloned capsaicin receptor integrates multiple pain-producing stimuli. Neuron *21*, 531-543.

28. Sasamura, T., Sasaki, M., Tohda, C., and Kuraishi, Y. (1998). Existence of capsaicin-sensitive glutamatergic terminals in rat hypothalamus. Neuroreport *9*, 2045-2048.

29. Mezey, E., Toth, Z.E., Cortright, D.N., Arzubi, M.K., Krause, J.E., Elde, R., Guo, A., Blumberg, P.M., and Szallasi, A. (2000). Distribution of mRNA for vanilloid receptor subtype 1 (VR1), and VR1-like immunoreactivity, in the central nervous system of the rat and human. Proceedings of the National Academy of Sciences of the United States of America *97*, 3655-3660.

30. Veronesi, B., Oortgiesen, M., Carter, J.D., and Devlin, R.B. (1999). Particulate matter initiates inflammatory cytokine release by activation of capsaicin and acid receptors in a human bronchial epithelial cell line. Toxicology and applied pharmacology *154*, 106-115.

31. Denda, M., Fuziwara, S., Inoue, K., Denda, S., Akamatsu, H., Tomitaka, A., and Matsunaga, K. (2001). Immunoreactivity of VR1 on epidermal keratinocyte of human skin. Biochemical and

biophysical research communications *285*, 1250-1252.

32. Cho, S., Lee, M.J., Kim, M.S., Lee, S., Kim, Y.K., Lee, D.H., Lee, C.W., Cho, K.H., and Chung, J.H. (2008). Infrared plus visible light and heat from natural sunlight participate in the expression of MMPs and type I procollagen as well as infiltration of inflammatory cell in human skin in vivo. J Dermatol Sci *50*, 123-133.

33. Park, C.H., Lee, M.J., Ahn, J., Kim, S., Kim, H.H., Kim, K.H., Eun, H.C., and Chung, J.H. (2004). Heat shock-induced matrix metalloproteinase (MMP)-1 and MMP-3 are mediated through ERK and JNK activation and via an autocrine interleukin-6 loop. J Invest Dermatol *123*, 1012-1019.

34. Shin, M.H., Moon, Y.J., Seo, J.E., Lee, Y., Kim, K.H., and Chung, J.H. (2008). Reactive oxygen species produced by NADPH oxidase, xanthine oxidase, and mitochondrial electron transport system mediate heat shock-induced MMP-1 and MMP-9 expression. Free Radic Biol Med *44*, 635-645.

35. Li, W.H., Lee, Y.M., Kim, J.Y., Kang, S., Kim, S., Kim, K.H., Park, C.H., and Chung, J.H. (2007). Transient receptor potential vanilloid-1 mediates heat-shock-induced matrix metalloproteinase-1 expression in human epidermal keratinocytes.

J Invest Dermatol *127*, 2328-2335.

36. Lee, Y.M., Li, W.H., Kim, Y.K., Kim, K.H., and Chung, J.H. (2008). Heat-induced MMP-1 expression is mediated by TRPV1 through PKCalpha signaling in HaCaT cells. Exp Dermatol *17*, 864-870.

37. Lee, Y.M., Kim, Y.K., Kim, K.H., Park, S.J., Kim, S.J., and Chung, J.H. (2009). A novel role for the TRPV1 channel in UV-induced matrix metalloproteinase (MMP)-1 expression in HaCaT cells. J Cell Physiol *219*, 766-775.

38. Lee, Y.M., Kang, S.M., and Chung, J.H. (2012). The role of TRPV1 channel in aged human skin. J Dermatol Sci *65*, 81-85.

39. Lee, Y.M., Kim, Y.K., and Chung, J.H. (2009). Increased expression of TRPV1 channel in intrinsically aged and photoaged human skin in vivo. Exp Dermatol *18*, 431-436.

40. Jin, K., Xie, L., Kim, S.H., Parmentier-Batteur, S., Sun, Y., Mao, X.O., Childs, J., and Greenberg, D.A. (2004). Defective adult neurogenesis in CB1 cannabinoid receptor knockout mice. Mol Pharmacol *66*, 204-208.

41. Alvarez-Figueroa, M.J., Pessoa-Mahana, C.D., Palavecino-Gonzalez, M.E., Mella-Raipan, J., Espinosa-Bustos, C., and

Lagos-Munoz, M.E. (2011). Evaluation of the membrane permeability (PAMPA and skin) of benzimidazoles with potential cannabinoid activity and their relation with the Biopharmaceutics Classification System (BCS). AAPS PharmSciTech *12*, 573-578.

42. Harkany, T., Keimpema, E., Barabas, K., and Mulder, J. (2008). Endocannabinoid functions controlling neuronal specification during brain development. Mol Cell Endocrinol *286*, S84-90.

43. Kupczyk, P., Reich, A., and Szepietowski, J.C. (2009). Cannabinoid system in the skin - a possible target for future therapies in dermatology. Exp Dermatol *18*, 669-679.

44. Berry, A., Bindocci, E., and Alleva, E. (2012). NGF, brain and behavioral plasticity. Neural Plast *2012*, 784040.

45. Lumpkin, E.A., and Caterina, M.J. (2007). Mechanisms of sensory transduction in the skin. Nature *445*, 858-865.

46. Nagahara, A.H., and Tuszynski, M.H. (2011). Potential therapeutic uses of BDNF in neurological and psychiatric disorders. Nat Rev Drug Discov *10*, 209-219.

47. Perez-Domper, P., Gradari, S., and Trejo, J.L. (2013). The growth factors cascade and the dendrito-/synapto-genesis versus cell survival in adult hippocampal neurogenesis: the chicken or the

egg. Ageing research reviews *12*, 777-785.

48. Volvert, M.L., Rogister, F., Moonen, G., Malgrange, B., and Nguyen, L. (2012). MicroRNAs tune cerebral cortical neurogenesis. Cell Death Differ *19*, 1573-1581.

49. Yu, H., and Chen, Z.Y. (2011). The role of BDNF in depression on the basis of its location in the neural circuitry. Acta Pharmacol Sin *32*, 3-11.

50. Adameyko, I., Lallemend, F., Aquino, J.B., Pereira, J.A., Topilko, P., Muller, T., Fritz, N., Beljajeva, A., Mochii, M., Liste, I., et al. (2009). Schwann cell precursors from nerve innervation are a cellular origin of melanocytes in skin. Cell *139*, 366-379.

51. Francis, N.J., and Landis, S.C. (1999). Cellular and molecular determinants of sympathetic neuron development. Annu Rev Neurosci *22*, 541-566.

52. Marchione, R., Kim, N., and Kirsner, R.S. (2009). Epidermal growth factor receptor regulates skin nerve outgrowth and branching. J Invest Dermatol *129*, 524.

53. Delcroix, G.J., Schiller, P.C., Benoit, J.P., and Montero-Menei, C.N. (2010). Adult cell therapy for brain neuronal damages and the role of tissue engineering. Biomaterials *31*, 2105-2120.

54. Fabbro, A., Villari, A., Laishram, J., Scaini, D., Toma, F.M., Turco, A., Prato, M., and Ballerini, L. (2012). Spinal cord explants use carbon nanotube interfaces to enhance neurite outgrowth and to fortify synaptic inputs. ACS Nano *6*, 2041-2055.

55. Gingras, M., Paradis, I., and Berthod, F. (2003). Nerve regeneration in a collagen-chitosan tissue-engineered skin transplanted on nude mice. Biomaterials *24*, 1653-1661.

56. McCarthy, B.G., Hsieh, S.T., Stocks, A., Hauer, P., Macko, C., Cornblath, D.R., Griffin, J.W., and McArthur, J.C. (1995). Cutaneous innervation in sensory neuropathies: evaluation by skin biopsy. Neurology *45*, 1848-1855.

57. Wang, L., Hilliges, M., Jernberg, T., Wiegleb-Edstrom, D., and Johansson, O. (1990). Protein gene product 9.5-immunoreactive nerve fibres and cells in human skin. Cell Tissue Res *261*, 25-33.

58. Schumacher, M.A., and Eilers, H. (2010). TRPV1 splice variants: structure and function. Front Biosci (Landmark Ed) *15*, 872-882.

59. Bhave, G., Hu, H.J., Glauner, K.S., Zhu, W., Wang, H., Brasier, D.J., Oxford, G.S., and Gereau, R.W.t. (2003). Protein kinase C phosphorylation sensitizes but does not activate the capsaicin receptor transient receptor potential vanilloid 1 (TRPV1). Proc

Natl Acad Sci U S A *100*, 12480-12485.

60. Jeske, N.A., Patwardhan, A.M., Ruparel, N.B., Akopian, A.N., Shapiro, M.S., and Henry, M.A. (2009). A-kinase anchoring protein 150 controls protein kinase C-mediated phosphorylation and sensitization of TRPV1. Pain *146*, 301-307.

61. Lee, J., Chung, M.K., and Ro, J.Y. (2012). Activation of NMDA receptors leads to phosphorylation of TRPV1 S800 by protein kinase C and A-Kinase anchoring protein 150 in rat trigeminal ganglia. Biochem Biophys Res Commun *424*, 358-363.

62. Mohapatra, D.P., and Nau, C. (2005). Regulation of Ca2+-dependent desensitization in the vanilloid receptor TRPV1 by calcineurin and cAMP-dependent protein kinase. J Biol Chem *280*, 13424-13432.

63. Zhang, X., Huang, J., and McNaughton, P.A. (2005). NGF rapidly increases membrane expression of TRPV1 heat-gated ion channels. EMBO J *24*, 4211-4223.

64. Carr, M.J., Kollarik, M., Meeker, S.N., and Undem, B.J. (2003). A role for TRPV1 in bradykinin-induced excitation of vagal airway afferent nerve terminals. J Pharmacol Exp Ther *304*, 1275-1279.

65. Ji, R.R., Samad, T.A., Jin, S.X., Schmoll, R., and Woolf, C.J.

(2002). p38 MAPK activation by NGF in primary sensory neurons after inflammation increases TRPV1 levels and maintains heat hyperalgesia. Neuron *36*, 57-68.

66. Light, A.R., Hughen, R.W., Zhang, J., Rainier, J., Liu, Z., and Lee, J. (2008). Dorsal root ganglion neurons innervating skeletal muscle respond to physiological combinations of protons, ATP, and lactate mediated by ASIC, P2X, and TRPV1. J Neurophysiol *100*, 1184-1201.

67. Ma, J., Altomare, A., Guarino, M., Cicala, M., Rieder, F., Fiocchi, C., Li, D., Cao, W., Behar, J., Biancani, P., et al. (2012). HCl-induced and ATP-dependent upregulation of TRPV1 receptor expression and cytokine production by human esophageal epithelial cells. Am J Physiol Gastrointest Liver Physiol *303*, G635-645.

68. Ma, J., Altomare, A., Rieder, F., Behar, J., Biancani, P., and Harnett, K.M. (2011). ATP: a mediator for HCl-induced TRPV1 activation in esophageal mucosa. Am J Physiol Gastrointest Liver Physiol *301*, G1075-1082.

69. Moriyama, T., Higashi, T., Togashi, K., Iida, T., Segi, E., Sugimoto, Y., Tominaga, T., Narumiya, S., and Tominaga, M. (2005). Sensitization of TRPV1 by EP1 and IP reveals peripheral

nociceptive mechanism of prostaglandins. Mol Pain *1*, 3.

70. Trevisani, M., Gazzieri, D., Benvenuti, F., Campi, B., Dinh, Q.T., Groneberg, D.A., Rigoni, M., Emonds-Alt, X., Creminon, C., Fischer, A., et al. (2004). Ethanol causes inflammation in the airways by a neurogenic and TRPV1-dependent mechanism. J Pharmacol Exp Ther *309*, 1167-1173.

71. Wu, Z.Z., and Pan, H.L. (2007). Role of TRPV1 and intracellular Ca2+ in excitation of cardiac sensory neurons by bradykinin. Am J Physiol Regul Integr Comp Physiol *293*, R276-283.

72. Zhuang, Z.Y., Xu, H., Clapham, D.E., and Ji, R.R. (2004). Phosphatidylinositol 3-kinase activates ERK in primary sensory neurons and mediates inflammatory heat hyperalgesia through TRPV1 sensitization. J Neurosci *24*, 8300-8309.

73. Vlachova, V., Teisinger, J., Susankova, K., Lyfenko, A., Ettrich, R., and Vyklicky, L. (2003). Functional role of C-terminal cytoplasmic tail of rat vanilloid receptor 1. J Neurosci *23*, 1340-1350.

74. Tominaga, M., and Tominaga, T. (2005). Structure and function of TRPV1. Pflugers Arch *451*, 143-150.

75. Yao, X., Kwan, H.Y., and Huang, Y. (2005). Regulation of TRP

channels by phosphorylation. Neurosignals *14*, 273-280.

76. Tominaga, M., Numazaki, M., Iida, T., Moriyama, T., Togashi, K., Higashi, T., Murayama, N., and Tominaga, T. (2004). Regulation mechanisms of vanilloid receptors. Novartis Found Symp *261*, 4-12; discussion 12-18, 47-54.

77. Chuang, H.H., Prescott, E.D., Kong, H., Shields, S., Jordt, S.E., Basbaum, A.I., Chao, M.V., and Julius, D. (2001). Bradykinin and nerve growth factor release the capsaicin receptor from PtdIns(4,5)P2-mediated inhibition. Nature *411*, 957-962.

78. Galoyan, S.M., Petruska, J.C., and Mendell, L.M. (2003). Mechanisms of sensitization of the response of single dorsal root ganglion cells from adult rat to noxious heat. Eur J Neurosci *18*, 535-541.

79. Stein, A.T., Ufret-Vincenty, C.A., Hua, L., Santana, L.F., and Gordon, S.E. (2006). Phosphoinositide 3-kinase binds to TRPV1 and mediates NGF-stimulated TRPV1 trafficking to the plasma membrane. J Gen Physiol *128*, 509-522.

80. Cayouette, S., and Boulay, G. (2007). Intracellular trafficking of TRP channels. Cell Calcium *42*, 225-232.

81. Osborne, R., Hakozaki, T., Laughlin, T., and Finlay, D.R. (2012).

Application of genomics to breakthroughs in the cosmetic treatment of skin ageing and discoloration. Br J Dermatol *166 Suppl 2*, 16-19.

82. Baumann, L. (2007). Skin ageing and its treatment. J Pathol *211*, 241-251.

83. Thom, E. (2005). A randomized, double-blind, placebo-controlled study on the clinical efficacy of oral treatment with DermaVite on ageing symptoms of the skin. J Int Med Res *33*, 267-272.

84. Palladino, P., Castelletto, V., Dehsorkhi, A., Stetsenko, D., and Hamley, I.W. (2012). Reversible thermal transition of polydiacetylene based on KTTKS collagen sequence. Chem Commun (Camb) *48*, 9774-9776.

85. Abu Samah, N.H., and Heard, C.M. (2011). Topically applied KTTKS: a review. Int J Cosmet Sci *33*, 483-490.

86. Tsai, W.C., Hsu, C.C., Chung, C.Y., Lin, M.S., Li, S.L., and Pang, J.H. (2007). The pentapeptide KTTKS promoting the expressions of type I collagen and transforming growth factor-beta of tendon cells. J Orthop Res *25*, 1629-1634.

87. Weisshaar, E., Kucenic, M.J., and Fleischer, A.B., Jr. (2003). Pruritus: a review. Acta Derm Venereol Suppl (Stockh), 5-32.

88. Szarvas, S., Harmon, D., and Murphy, D. (2003). Neuraxial opioid-induced pruritus: a review. J Clin Anesth *15*, 234-239.

89. Denman, S.T. (1986). A review of pruritus. J Am Acad Dermatol *14*, 375-392.

90. Lyell, A. (1972). The itching patient. A review of the causes of pruritus. Scott Med J *17*, 334-337.

91. Chambers, G.O. (1945). A Review on Pruritus Ani. Postgrad Med J *21*, 151-158.

92. Akiyama, T., Tominaga, M., Takamori, K., Carstens, M.I., and Carstens, E. (2013). Roles of glutamate, substance P, and gastrin-releasing peptide as spinal neurotransmitters of histaminergic and nonhistaminergic itch. Pain.

93. Smith, E.S., Blass, G.R., Lewin, G.R., and Park, T.J. (2010). Absence of histamine-induced itch in the African naked mole-rat and "rescue" by Substance P. Mol Pain *6*, 29.

94. Hosokawa, C., Takeuchi, S., and Furue, M. (2009). Severity scores, itch scores and plasma substance P levels in atopic dermatitis treated with standard topical therapy with oral olopatadine hydrochloride. J Dermatol *36*, 185-190.

95. Andoh, T., and Kuraishi, Y. (2006). Suppression by bepotastine

besilate of substance P-induced itch-associated responses through the inhibition of the leukotriene B4 action in mice. Eur J Pharmacol *547*, 59-64.

96. Kamo, A., Negi, O., Tengara, S., Kamata, Y., Noguchi, A., Ogawa, H., Tominaga, M., and Takamori, K. (2013). Histamine H Receptor Antagonists Ineffective against Itch and Skin Inflammation in Atopic Dermatitis Mouse Model. J Invest Dermatol.

97. Rukwied, R.R., Main, M., Weinkauf, B., and Schmelz, M. (2013). NGF sensitizes nociceptors for cowhage- but not histamine-induced itch in human skin. J Invest Dermatol *133*, 268-270.

98. Wilson, S.R., Gerhold, K.A., Bifolck-Fisher, A., Liu, Q., Patel, K.N., Dong, X., and Bautista, D.M. (2011). TRPA1 is required for histamine-independent, Mas-related G protein-coupled receptor-mediated itch. Nat Neurosci *14*, 595-602.

99. Akiyama, T., Carstens, M.I., and Carstens, E. (2010). Enhanced scratching evoked by PAR-2 agonist and 5-HT but not histamine in a mouse model of chronic dry skin itch. Pain *151*, 378-383.

100. Andoh, T., Al-Akeel, A., Tsujii, K., Nojima, H., and Kuraishi, Y. (2004). Repeated treatment with the traditional medicine Unsei-in

inhibits substance P-induced itch-associated responses through downregulation of the expression of nitric oxide synthase 1 in mice. J Pharmacol Sci *94*, 207-210.

101. Patel, K.N., Liu, Q., Meeker, S., Undem, B.J., and Dong, X. (2011). Pirt, a TRPV1 modulator, is required for histamine-dependent and -independent itch. PLoS One *6*, e20559.

102. Kim, S.J., Park, G.H., Kim, D., Lee, J., Min, H., Wall, E., Lee, C.J., Simon, M.I., Lee, S.J., and Han, S.K. (2011). Analysis of cellular and behavioral responses to imiquimod reveals a unique itch pathway in transient receptor potential vanilloid 1 (TRPV1)-expressing neurons. Proc Natl Acad Sci U S A *108*, 3371-3376.

103. Alenmyr, L., Hogestatt, E.D., Zygmunt, P.M., and Greiff, L. (2009). TRPV1-mediated itch in seasonal allergic rhinitis. Allergy *64*, 807-810.

104. Gazzieri, D., Trevisani, M., Springer, J., Harrison, S., Cottrell, G.S., Andre, E., Nicoletti, P., Massi, D., Zecchi, S., Nosi, D., et al. (2007). Substance P released by TRPV1-expressing neurons produces reactive oxygen species that mediate ethanol-induced gastric injury. Free Radic Biol Med *43*, 581-589.

105. Andoh, T., Nagasawa, T., Satoh, M., and Kuraishi, Y. (1998).

Substance P induction of itch-associated response mediated by cutaneous NK1 tachykinin receptors in mice. J Pharmacol Exp Ther *286,* 1140-1145.

106. Ruiz-Villaverde, R., and Sanchez-Cano, D. (2009). [Idiopathic senile pruritus: therapeutic response to gabapentin]. Rev Esp Geriatr Gerontol *44,* 355-356.

107. Bernhard, J.D. (1997). Do anti-basement membrane zone antibodies cause some cases of 'senile pruritus'? Arch Dermatol *133,* 1049-1050.

108. Steigleder, G.K. (1986). [Senile pruritus]. Z Hautkr *61,* 261-262.

109. Li, Y., Liu, Y., Xu, Y., Voorhees, J.J., and Fisher, G.J. (2010). UV irradiation induces Snail expression by AP-1 dependent mechanism in human skin keratinocytes. J Dermatol Sci *60,* 105-113.

110. Huang, C., Zhang, D., Li, J., Tong, Q., and Stoner, G.D. (2007). Differential inhibition of UV-induced activation of NF kappa B and AP-1 by extracts from black raspberries, strawberries, and blueberries. Nutr Cancer *58,* 205-212.

111. Djavaheri-Mergny, M., and Dubertret, L. (2001). UV-A-induced AP-1 activation requires the Raf/ERK pathway in human NCTC

2544 keratinocytes. Exp Dermatol *10*, 204-210.

112. Lee, M., Kim, J.Y., and Anderson, W.B. (2004). Src tyrosine kinase inhibitor PP2 markedly enhances Ras-independent activation of Raf-1 protein kinase by phorbol myristate acetate and H2O2. J Biol Chem *279*, 48692-48701.

113. Stokoe, D., and McCormick, F. (1997). Activation of c-Raf-1 by Ras and Src through different mechanisms: activation in vivo and in vitro. EMBO J *16*, 2384-2396.

114. D'Arcangelo, G., and Halegoua, S. (1993). A branched signaling pathway for nerve growth factor is revealed by Src-, Ras-, and Raf-mediated gene inductions. Mol Cell Biol *13*, 3146-3155.

115. Xing, B.M., Yang, Y.R., Du, J.X., Chen, H.J., Qi, C., Huang, Z.H., Zhang, Y., and Wang, Y. (2012). Cyclin-dependent kinase 5 controls TRPV1 membrane trafficking and the heat sensitivity of nociceptors through KIF13B. J Neurosci *32*, 14709-14721.

116. Kopylova, L.V., Snytnikova, O.A., Chernyak, E.I., Morozov, S.V., and Tsentalovich, Y.P. (2007). UV filter decomposition. A study of reactions of 4-(2-aminophenyl)-4-oxocrotonic acid with amino acids and antioxidants present in the human lens. Exp Eye Res *85*, 242-249.

117. Damiani, E., Baschong, W., and Greci, L. (2007). UV-Filter combinations under UV-A exposure: concomitant quantification of over-all spectral stability and molecular integrity. J Photochem Photobiol B *87*, 95-104.

118. Bollmann, F., Casper, I., Henke, J., and Pautz, A. (2012). qRT-PCR: a method and its difficulties. Naunyn Schmiedebergs Arch Pharmacol *385*, 949-951.

119. Zhang, T., Shao, M.F., and Fang, H.H. (2009). A qRT-PCR-based method for the measurement of rrn operon copy number. Lett Appl Microbiol *49*, 26-30.

120. Maksymowicz-Mazur, W., Pendzich, J.B., Mazurek, U., Wilczok, A., Dworniczak, S., Kozielski, J., and Oklek, K. (2003). [Detection of 85B mRNA in Mycobacterium tuberculosis cultures using the quantitative QRT-PCR (TaqMan) method]. Wiad Lek *56*, 419-424.

121. Byun, H.J., Cho, K.H., Eun, H.C., Lee, M.J., Lee, Y., Lee, S., and Chung, J.H. (2012). Lipid ingredients in moisturizers can modulate skin responses to UV in barrier-disrupted human skin in vivo. J Dermatol Sci *65*, 110-117.

122. Lee, Y.M., Kang, S.M., Lee, S.R., Kong, K.H., Lee, J.Y., Kim, E.J., and Chung, J.H. (2011). Inhibitory effects of TRPV1 blocker on

UV-induced responses in the hairless mice. Arch Dermatol Res *303*, 727-736.

123. Jones, R.R., Castelletto, V., Connon, C.J., and Hamley, I.W. (2013). Collagen stimulating effect of peptide amphiphile C16-KTTKS on human fibroblasts. Mol Pharm *10*, 1063-1069.

124. Palladino, P., Castelletto, V., Dehsorkhi, A., Stetsenko, D., and Hamley, I.W. (2012). Conformation and self-association of peptide amphiphiles based on the KTTKS collagen sequence. Langmuir *28*, 12209-12215.

125. El-Hashim, A.Z., and Jaffal, S.M. (2009). Nerve growth factor enhances cough and airway obstruction via TrkA receptor- and TRPV1-dependent mechanisms. Thorax *64*, 791-797.

126. Xing, J., Lu, J., and Li, J. (2009). Contribution of nerve growth factor to augmented TRPV1 responses of muscle sensory neurons by femoral artery occlusion. Am J Physiol Heart Circ Physiol *296*, H1380-1387.

127. Bernhard, J.D. (1992). Phantom itch, pseudophantom itch, and senile pruritus. Int J Dermatol *31*, 856-857.

국문 초록

Transient receptor potential vanilloid 1 (TRPV1)는 캡사이신, 열, 자외선, 산성 **pH** 등의 물리-화학적 자극에 의해 활성화되는 비선택적 양이온 채널이다. 신경세포에서 **TRPV1** 채널 활성화는 세포막 탈분극과 칼슘유입을 일으켜서 통증자극을 매개하는 것으로 잘 알려져 있다. **TRPV1** 채널은 신경 세포뿐만 아니라 각질형성화 세포에서도 발현된다는 것이 알려져 있으나, 피부에서 **TRPV1** 채널의 생리학적 역할에 대한 연구는 부족하다. 최근 우리 연구실에서는 **TRPV1** 채널이 피부의 광노화 및 내인성 노화에 관련됨을 제시한 바 있다. 즉, 열이나 자외선과 같은 피부노화유발 자극원에 의해 피부세포에서 **TRPV1**이 활성화될 뿐만 아니라 발현이 증가됨을 보였다.

이를 바탕으로 본 연구에서는 **TRPV1**이 자외선에 의해 활성화되는 신호기전을 조사하였고, 자외선에 의하여 **TRPV1**의 세포질에서 세포막으로의 이동이 증가하며 이 단계에 **Src kinase**가 관여함을 인체 각질형성세포주 **(HaCaT)**에서 규명하였다.

또한 **TRPV1** 채널을 타겟으로 하여 피부노화를 억제할 수 있는 방안으로서 **TRPV1** 억제성 펩타이드를 고안하였고, **TRPV1** 억제성

펩타이드가 자외선이나 열에 의한 **MMP-1** 단백질 및 **mRNA**의 발현을 억제함을 **HaCaT** 세포에서 규명하였다. 실제 생체에서의 적용가능성을 알아보기 위하여, 무모쥐를 이용하여 **TRPV1** 억제성 펩타이드가 자외선에 의한 피부두께 증가 및 **MMP-13**과 **MMP-9**의 발현 및 세포자살을 억제함을 확인하였다.

마지막으로, **TRPV1**이 노인 피부에서 증가된다는 선행 결과를 바탕으로 하여, **TRPV1**이 원래 발견되었던 신경세포의 관련 유전자들이 내인성 노화과정에서 피부조직에서도 증가할 가능성을 조사하였고, 다수의 신경관련 표지단백의 발현 증가를 확인하였다. 특히 **substance P** 수용체와 **TRPV1**의 발현증가는 노인성 소양증에서 **TRPV1**이 관여할 가능성을 시사한다.

이와 같은 연구 결과는 피부에 존재하는 **TRPV1** 채널이 광노화 및 내인성 노화를 억제하기 위한 방안 모색에서 중요하고 효과적인 표적임을 제시한다.

주요어 : **TRPV1**, 내인성 노화, 신경세포 관련 유전자, 자외선에 의한 광노화 반응, **TRPV1** 억제성 펩타이드, **Src kinase**

학 번 : **2010-30603**

감사의 글

우선, 이렇게 좋으신 지도 교수님을 만나게 해주시고 좋은 여건 가운데서, 한없이 정교하고 놀라운 신비를 담은 학문인 생명과학을 탐구할 수 있도록 인도해주신 하나님께 감사드립니다.

2009년 10월에 우연히 '늙지않는 피부, 젊어지는 피부' 라는 책을 통해 정진호 선생님을 처음 알게 되었는데, 어느덧 4년이라는 시간이 훌쩍 흘러 제가 선생님의 제자로 박사학위를 받게 되는 날이 오게 되다니 여러 가지로 가슴이 벅차 오릅니다. 책에서만큼이나 늘 연구에 그 누구보다 열정적이신 모습으로 본을 보여 주시며, 바쁘신 가운데에도 언제나 자상하게 신경 써주시고 마음껏 연구하고 공부할 수 있도록 배려해 주신 정진호 선생님께 진심으로 감사드립니다. 선생님의 모습을 통해 진정학 과학도로서의 길이 무엇인지 잘 배울 수 있었던 것 같습니다.

석사과정 때뿐만 아니라 박사과정 동안에도 늘 세심하게 가르쳐주시고 지도해주신 박동은 선생님을 비롯하여, 부족한 저의 학위 논문을 심사해주시고 성심 성의로 지도해주신 김규한 교수님, 김성준 교수님, 오상호 교수님께도 감사를 드립니다. 열정이 어떠한 것인지를 몸소 보여주신 권오상 교수님께도 감사드립니다. 늘 인자한 미소로 응원해주신 서인석 교수님과 멋진 과학자의 길을 걷고 계신 김총호 교수님께도 감사드립니다.

4년이라는 시간 동안 함께 연구실 생활을 하며 감사드릴 분들이 참 많습니다. 우선 짧은 시간이었지만 많은 것을 가르쳐주신 이영미 박사님께 감사드립니다. 또한 언제나 인자하고 자상한 모습으로 지도해주신 이동훈 박사님과 오장희 박사님께도 진심으로 감사드립니다. 졸업한 후에도 언제나 함께 있는 것처럼 힘을 주는 정윤이, 늘 한결 같은 모습으로 열심인 민경이, 저에게 정말 속깊은 정으로 늘 용기 주셨던 지은언니와 인경언니, 늘 본이 되면서도 은근한 애교가 넘치는 슈퍼우먼 현선언니께도 감사드립니다.

1년동안 좋은 체력 아끼지 않고 정말 열심히 함께 실험 도와준 상범이, 임상 실험을 하는데 적극적으로 도와주신 이정숙 간호사님과 동물실험 때 늘 큰 도움 주신 신창엽 선생님과 동물실험 염색 힘써 도와주신 연경언니께도 감사드립니다. 또한 언제나 과학도로서의 본을 보이시며 변함없는 열심으로 연구하시는 박치헌 박사님, 신미희박사님, 김민경 박사님, 김은주 박사님, 서은영 박사님, 조애리 박사님께도 감사드립니다. 또한 같은 길을 걸으며 같은 공간에서 함께 힘이 되어준 정수오빠, 선필오빠, 요성, 성수, 미라, 경현, Novi, 김승룡 선생님에게도 감사합니다. 짧지 않은 시간 동안 연구실 생활을 잘 할 수 있도록 도와주신 민정언니, 세라언니, 순진언니, 선영언니, 이영애 선생님, 김은희 선생님, 윤지선박사님, 장선혜박사님께도 감사드립니다.

마지막으로 공부에만 집중할 수 있도록 항상 곁에서 기도로 응원해주신 사랑하는 저희 가족들에게 감사드립니다. 막내딸 노릇도 잘 못하는 딸을 위해 매일같이 기도해주시고 이해해주시는 부모님과 언제나 지혜롭게 아낌없는 조언을 주는 유민언니, 친구같이 편하지만 언제나 멋지고 착한 혜민언니, 그 삶 자체가 너무너무 존경스러운 최고의 남편상인 형부께도 감사드립니다. 학위 심사 받는 동안 예민해진 저를 위해 기도와 맛있는 양식으로 늘 응원해주며 힘이 되어준 최고 멋진 호준오빠, 늘 재치 넘치는 입담과 맛집으로 위로와 웃음을 준 봉균오빠, 곁에서 항상 위로가 되어주는 소중한 내 친구들, 서연이, 민희, 지영이, 수진이, 희진이, 선미, 윤이, 혜인이, 그리고 대화를 나눌수록 힘이 되어주는 지원이, 내 죽마고우 멋진 커리어 우먼 윤영이, 같은 길을 걷는 귀여운 동창 주은이, 늘 듬직하고 각자의 자리에서 멋지게 해내고 있는 선영이, 동건이, 상훈이, 또 늘 힘이 되어준 디사이플 콰이어 가족들, 특히 지영이, 은혜, 유리, 수정이, 지현언니, 현정언니께도 감사드립니다.

앞으로도 이 모든 은혜에 힘입어 더욱 성숙하고 뿌리깊은 과학도로서의 길을 걸어가도록 노력하겠습니다. 다시 한번 박사 학위를 받기까지 도와주신 모든 분들께 감사드립니다.